Available online at www.CivileJournal.org

Civil Engineering Journal

(E-ISSN: 2476-3055; ISSN: 2676-6957)

Vol. 8, No. 04, April, 2022

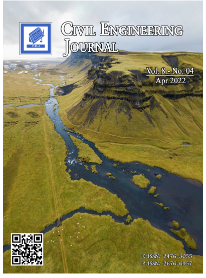

The Effect of Shear Wall Openings on the Response Reduction Factor

Nasr E. Nasr [1], M. N. Fayed [1], Gamal Hussien [1], A. M. El-Makhlasawi [1*]

[1] *Dept. of Structural Engineering, Faculty of Engineering, Ain-Shams University, Cairo 11757, Egypt.*

Received 19 December 2021; Revised 19 March 2022; Accepted 25 Marh 2022; Published 01 April 2022

Abstract

This research attempts to investigate the effect of shear wall openings on the response reduction factor. Openings are commonly necessary because of other engineering disciplines' requirements. When openings are modest in proportion to the size of the wall, their effects are frequently disregarded. On the other hand, when these openings are large or located in a high-risk area, they can have a significant impact. A broad literature review has been conducted in the present study. A verified comparative example consisting of eight stories was studied. Then, a numerical study has been conducted on two different model sets with 16 and 8 stories, which were designed according to the Egyptian code of loads, ECP-201 (2012), and checked according to the Euro code, EC8 (2004). ETABS software was used to conduct pushover analysis before and after applying different-sized openings. The ground-opening effect has also been studied. The results show that by increasing the opening area, the R-factor was reduced. It is more influenced by the opening height than the width, though. By increasing the number of stories, the reduction percentage in the R-Factor increased for openings that are less than 30% of the wall area. The R-factor increases slightly when half of the reinforcement bars are added.

Keywords: Reduction/Modification Factor (R); Pushover Analysis; Nonlinear Static Analysis; Shear Walls with Openings; Spandrel; Coupled Wall; Modelling; Dual System; Multi-Story Buildings.

1. Introduction

Wind and earthquake loads have different design requirements than gravity (dead and live) loads. Due to the frequency of loading conditions, wind loads are a primary requirement. Structures in high-seismic locations are built to endure lateral movements as well. Structures are normally built to withstand lateral wind loads that represent about 1% to 3% of their total weight. However, earthquake loads can reach 30–40 percent of the structure's weight, which may result in extraordinarily heavy and expensive structures if the same elastic design principles were used. As a result, the concepts of controlled damage and collapse prevention are used in earthquake design, and the R-factor's importance appears clearly.

Reinforced concrete structural shear walls have long been known as one of the most effective lateral force resisting techniques for buildings subjected to earthquakes and wind. Their high stiffness can reduce or eliminate damage to nonstructural components, and they can provide enough strength to withstand moderate to intense ground shaking with just minor structural damage. The implementation of openings in shear walls is frequently required as a result of other engineering disciplines' needs. When the openings are small in comparison to the wall dimensions, their impacts are often overlooked [1]. When these openings are quite wide or placed in a critical region, however, they can have a significant impact on the seismic performance of RC walls. "Coupled walls" are shear walls with openings, as shown in

* Corresponding author: eng_elmakhlasawi@yahoo.com

http://dx.doi.org/10.28991/CEJ-2022-08-04-013

Figure 1. These walls act as cantilevered walls with coupling beams connecting them. For bending and shearing effects, coupling beams might be a spandrel or lintel. These openings indicate a weak region through which the fracture might pass due to its low stiffness and may lead to failure as shown in Figures 2 to 4. So, the value of the modification factor may be affected by these openings.

Many researchers have conducted experimental and finite element investigations to illustrate the influence of these openings. The majority of these studies on shear walls with openings focused on the relationship between opening features and displacement, rather than the influence of these opening parameters on the response reduction-modification factor (R). As a result, there was a strong desire to discover how these openings would affect the R-factor and hence the design. The Egyptian code hadn't mentioned any factor that could be used to take into consideration the impact of these openings and be satisfied with a fixed factor for buildings that have shear wall systems. In this research, the influence of these openings on the R-factor is clarified and calculated using nonlinear behavior.

Nonlinear pushover analysis is applied to a finite element model designed according to the ECP-201 (2012) [2] using a finite element program ETABS [3] to determine the (R) factor value. An eight-stories building has been modelled using ETABS and SAP2000 [4] software. Walls are defined as fiber- and layered-shell elements in these models. Then, a pushover analysis was conducted. The results were concluded and compared with the original paper results [5]. A numerical study was carried out for two different limited ductility buildings, which have been well designed for ground motions, $A_g/g = 0.25$, spectrum type (1), according to the Egyptian code. Then, pushover analysis was conducted on the two models with 16 and 8 stories without openings, and after applying different sizes of openings to every model to assess the effect of the openings' area, width, height, and number of stories on the (R) factor. The lintel beam above the opening has been defined by two different methods. The difference between defining a lintel beam as a wall segment or a spandrel has been clarified. In addition, half of the reinforcement bars that had been cut to conduct openings have been added on either side of the opening to explore its influence on the R-factor. The results are discussed, and recommendations are given.

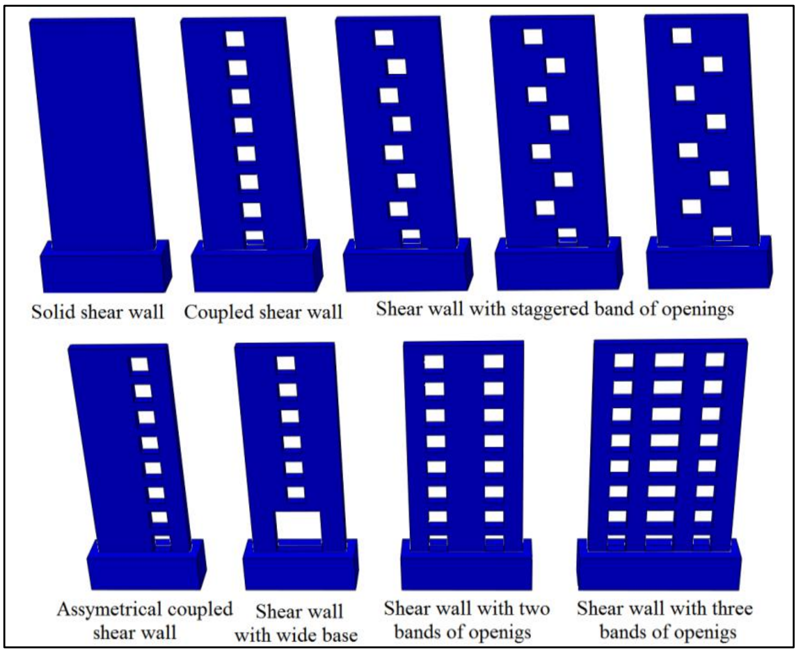

Figure 1. Typical types of shear walls [6]

Figure 2. Damage at the discontinuity [7]

Figure 3. Pier and Spandrel Failure [7]

Figure 4. Coupling Beam Failure [8]

2. Research Methodology

This study aims to present the impact of shear wall openings on the R-factor and its relation to the value mentioned in the Egyptian code. It shows the flowchart of all the steps to achieve its objective. Firstly, data is collected from different sources. Then, a literature review concerning the subject is conducted, the different methods of evaluating the R-factor are reviewed, and study models are chosen. Finally, the results of the research are presented, and a conclusion is obtained.

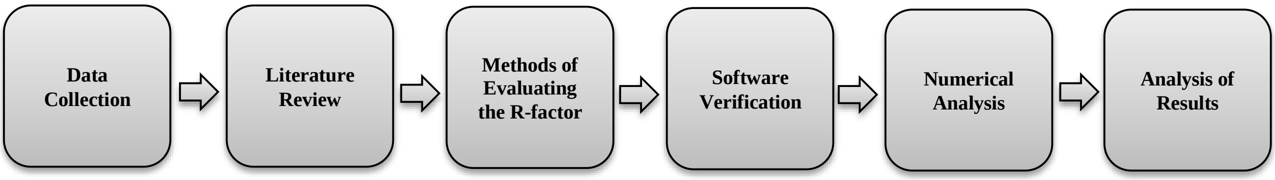

Figure 5. Flowchart of the research methodology

3. Previous Studies on RC Shear Walls with Openings

Many literature reviews were conducted for shear walls with different types of openings, different in geometry, locations, usage, and arrangement. Most of these studies dealt mainly with the effect of the previously mentioned types on the base shear. Table 1 illustrates some of these studies and summarizes their major findings.

Table 1. Previous Research on Shear Walls with Openings, Variables, and Major Findings

Author	Type of Study	Variables of the research	Main findings
Khatami et al. (2012) [9]	Finite element simulation (ANSYS software)	Deflection, Bending moment, Shearforce and the consequences of openings in concrete shear walls.	• Opening decreases lateral carrying capacities of shear walls. • Shear walls have a delay in opening deformation as compared to the whole panel at the yielding load level. • The behavior and performance of shear walls with openings, decreasing their role in lateral load-carrying capacity.
Chowdhury et al. (2012) [10]	Finite element simulation (ETABS software)	The behaviour of a shear wall containing an opening when subjected to seismic loads.	• The larger the opening, the more displacements the building allows, and this tendency continues as the storey level rises. In terms of displacement at the topmost storey level, thickening the wall around door openings is more effective than that around window openings. Furthermore, opening in the shear wall in plane of loading is more essential than opening in the shear wall out of the plane of loading since there is a considerable shift in displacement following opening in the shear wall in the plane of loading.

Rajesh et al. (2014) [11]	Finite element simulation (SAP2000 software)	The seismic behavior of this shear wall such as aspect ratio of walls, reinforcement detailing aspects, and presence of openings.	• Improve ductile detailing in lower 2 stories by using boundary elements improves the wall base shear capacity and the ductility. • Presence of openings reduces the shear capacity and causes a reduction of the post-yield stiffness and decreases the deformation capacity of the wall. • Decrease the aspect ratio of the shear-wall decreases the base shear capacity of the building.
Itware & Kalwane (2015) [12]	Finite element simulation (STAAD PRO software)	The effects of openings in shear wall on seismic response of structures.	• The size of openings, rather than their placement in the shear walls, affects the stiffness of the shear wall structure for opening areas less than 20% of the shear wall area. The stiffness of the system is considerably impacted by the placement of openings in shear walls when the opening area exceeds 20% of the shear wall area. The effects of horizontal placement of door openings of 1×2.1 m on the stiffness of the system may be ignored. However, the stiffness of the system is substantially affected by the vertical placement of the window opening.
Sharma et al. (2015) [13]	Finite element simulation	Different types of openings in shear walls, Volume of reduction in the shear wall due to openings.	• Displacement and drift are not only dependent on the size of the opening, but the shape of the opening also plays a major role when the aspect ratio is large. The overall lateral displacement of the buildings increases from 0.58 % to 20.95 % and inter-storey drift increases about 1.04 % to 23.63 % because various sizes of openings in shear walls are provided in comparison to shear walls without openings. • Reduction in shear wall volume due to opening is incorporated by increasing the size of the adjacent boundary elements, stiffness tends to increase compared to the first case. Thus, overall lateral displacement and inter-storey drift of the buildings decrease by 0.13 % to 17.65 % and 0.34 % to 21.45 % respectively as compared to the first case.
Gandhi et al. (2015) [14]	Finite element simulation (STAAD PRO software)	The effect of size and location of the openings in shear walls.	• There is a direct correlation between the opening percentage and the deflection. • Opening increases bottom Stresses around the opening. • When the percent of opening exceeds 40% the deflection and stresses around opening increase more rapidly. • Eccentric zigzag with a 20% opening has a lower deflection than Eccentric Straight, which has the highest deflection, and concentric loading has a lower deflection than Eccentric Straight.
Kankuntla et al. (2016) [15]	Finite element simulation (SAP software)	The performance of a shear wall with an opening in the middle.	• The existence of openings in a shear wall reduces the shear wall's strength and rigidity. • Because the rigidity of the shear wall with openings diminishes, the column moment and axial force rise as the size of the opening increases. • As the length of the shear wall in the plan rises, the opening impact decreases, and the form of the opening dose not influence the structure's reactions, but the height and breadth of the apertures do. • The stiffness and responsiveness of structures with opening areas less than 15% are impacted by the size of openings rather than their placements. However, opening sites in shear walls with opening areas of more than 15% have a significant impact.
Jagadale et al. (2016) [16]	Finite element simulation (ETABS software)	The performance and the behaviour of vertical and staggered opening.	• The staggered opening had a better performance than the vertical. The base shear is less for the staggered openings. The base shear without opening is more as compared to opening and also observe that the time period is more with a comparison of vertical opening without opening.
Khatavkar et al. (2017) [17]	Finite element simulation (ETABS software)	Vertical and staggered opening arrangements effect on the efficacy of shear walls.	• In terms of displacement, storey drift, and storey shear, a regular structure with a shear wall with a staggered opening produces superior results. Structures with staggered openings offer superior outcomes in terms of displacement, storey drift, and storey shear in both directions in the case of irregular buildings (H-shaped and T-shaped). However, in the instance of an L-shaped irregular structure with vertical openings, the displacement and base shear in the Y-direction were both satisfactory.
Swetha et al. (2017) [18]	Finite element simulation (ETABS software)	Base shear, storey displacement, storey drift, storey acceleration, and time period	• The timing, displacement, drift, base shear, and overall seismic response of the structure are all affected by the opening position. • Shear wall with staggered apertures has 1.25 percent lower base shear than a shear wall with vertical openings and 3.67 percent lower base shear than shear wall with horizontal openings. • Shear wall with staggered apertures demonstrated 1.35 percent greater time period and storey acceleration than a shear wall with openings oriented vertically and horizontally, and about 3% higher than a shear wall without openings.

Hosseini (2017) [19]	Finite element simulation (ETABS software)	Shear walls cases with openings and Without openings	• Shear walls could decrease the shear force in the columns and increase the moment in the columns. • No significant difference in shear force and moment provision of 20% opening in the shear wall.
Zhang (2018) [20]	Finite element simulation (ABAQUS software)	The effect of the openings on the performance of the wall panels	• It is recommended to keep the locations of the openings closer to the neutral axis to design the walls with circular openings. • The spacing between the flexural and shear reinforcements could be decreased to improve the moment and shear capacities of the wall. • A higher-strength concrete could be used to provide the wall with a higher axial loading capacity.
Yadav et al. (2019) [21]	Finite element simulation (ETABS software)	The location and types of openings in shear walls	• It is observed that deflection, Bending Moment ,and Shear Force increases as the size of the opening increases. • The opening should be of minimum size and number as the height of the structure goes on increasing.
Alimohammadi et al. (2019) [22]	Finite element simulation (ABAQUS software)	Shear wall has a constant cross-section by applying different shapes of opening square, circular and rectangular.	• Opening affects the resistance/hardening of the models. • Strength decreased by decreasing the distance between the opening and the wall edge. • Opening could reduce the seismic properties of the shear wall up to 50 percent on the stiffness, ultimate load, and energy absorption, but the strength and ductility of the reduction are variable depending on the type and form of openings.
Ma'moun (2020) [23]	Finite element simulation (ETABS software)	The R-factor of RC structures with shear walls with different sizes of openings.	• An increase in the storey height by 11% causes a decrease in the RMF value by 10%. • The ratio between opening sizes to the area of the shear walls affects the RMF. • The decrease is compensated with the ductility in shear walls with openings by redesigning the boundary elements in shear walls. • Openings affect the maximum base shear and the maximum displacement that causes a decrease in the RMF values, due to the reduction in the Rs and Rμ.
Varma et al. (2021) [24]	Finite element simulation (ETABS software)	The effect of openings on the storey drift, stiffness, and stresses.	• When the opening is located at a higher storey level, the total deflection decreased. • The ground storey has the maximum total deflection. • Total displacements are higher when openings are supplied towards the edges of the walls than when openings are placed in the centre of the wall. • When compared to shear walls placed in the middle of the bay, providing shear walls at the corners of the frame produces good results.
Zhang et al. (2022) [25]	Experimental and Finite element simulation (ABAQUS software)	The effect of openings arrangement on the failure mode, ultimate loading capacities, energy dissipation capacities, and stresses.	• The placement of openings has a clear impact on the residual ductility of post-opening RC shear walls. • Opening many holes vertically is preferable to opening multiple holes horizontally. • Post holes drastically limit the shear wall's energy dissipation capability. • The location of post-openings has an impact on the shear wall's failure mode. • The vertical reinforcement near the opening bear's greater stress.
Fares (2021) [26]	Finite element simulation (SAP2000)	The effect of openings on the lateral stiffness.	• Enhance the size of the openings at shear walls to increase lateral displacement and hence reduce the structure's lateral stiffness. • When 5% of the stiffness ratio RS decrease may be permitted, the greatest window opening at concrete shear walls that can be overlooked in modelling owing to simplification is determined to be up to 3% of the total wall area. • The influence of openings on lateral deflection and stiffness can be reduced by raising the wall aspect ratio H/B. • A typical door in normal usage with dimensions of 1.00 x 2.00m reduces the rigidity of a 3×3m solid wall by 60%.

4. Concept For Determining Response Modification Factor (R)

In the past, it was useless to design buildings to withstand earthquakes and wind. Most structures were constructed just for gravity loads (dead and live), but there is now an urgent need to consider lateral loads as well. The design criteria for lateral loads differ significantly from those for gravity loads. Lateral loads are less likely to occur. As a result, designing a structure to bear lateral force at the elastic performance level will not be cost-effective. In particular, earthquake loads can reach 30:40 percent of the structure's weight, compared to only 1:3 percent for wind loads. Inelastic performance levels of controlled damage and collapse prevention should be considered as a result.

The main seismic design tool, response modification factors (R), shows the predicted inelasticity level in structural systems. The R factor has many different definitions and names according to the various codes, IS 1893 (Part 1): (2002) [27] defines R as "*response reduction factor*", ASCE 7:(2005) [28] defines it as "*response modification coefficient*", the Euro code - 8 [29] defines it as "*behavior factor*" (q), and the Egyptian code ECP-201 (2012) [2] defines it as "response modification factor (R-factor)". R factor mirrors the ability of a structure to dissipate energy through inelastic performance levels and is used to reduce the design forces that enable us to have an economical structure. The factor accounts for the nonlinear response of a structure by taking advantage of the fact that structures possess significant reserve strength and capacity to dissipate energy, called over strength and ductility, respectively (ATC (1995a) [30], Borzi & Elnashai (2000) [31], Rahem et al. (2021) [32]).

The values assigned to the response modification factor (R) of the US-codes, FEMA [33-35]; UBC1997, aim to account for reserve strength and ductility too (ATC, 1995) [30]. ATC-19 calculates the R-factor as an equation of three parameters that affect the seismic response of the structure (ductility, over strength, and redundancy).

The ductility reduction factor (Rμ), which decreases the elastic demand force to the maximum yield strength of the structure, and the over-strength factor (Ω), which accounts for the over-strength introduced in code-designed buildings, are the major reasons for such substantial reductions. As a result, the R-factor as follows:

$$R = R\mu \times \Omega \tag{1}$$

The relationship between the base-shear of a structure and its roof displacement, which can be calculated by a nonlinear static analysis, has been illustrated in Figures 6 and 7.

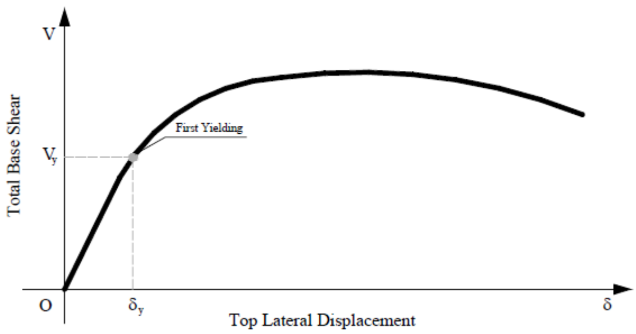

Figure 6. Yield definition as a first yield [36]

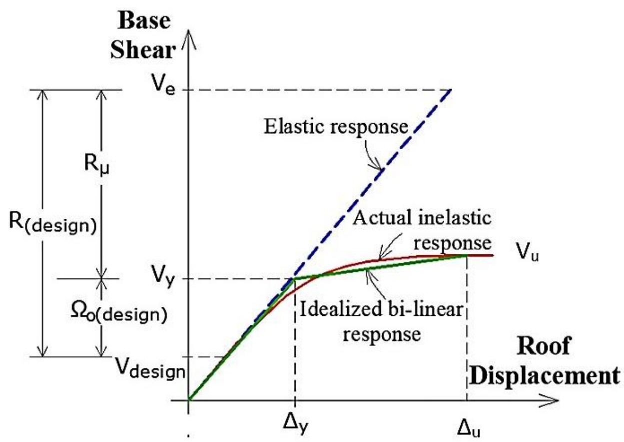

Figure 7. Force displacement response of elastic and inelastic systems

4.1. Over-Strength Factor Ω

The over-strength factor (Ω) can be defined as the ratio of the actual to design level strength [37]. It can be expressed as:

$$\Omega = Vy / Vd \tag{2}$$

where Vy is the actual strength and Vd is the design strength.

4.2. Ductility Reduction Factor, Rμ

The extent of inelastic deformation experienced by the structural system subjected to a given ground motion or lateral loading is given by the displacement ductility ratio "μ" [38]. The inelastic behaviors of a structure can be idealized as:

$$\mu = \Delta u / \Delta y \tag{3}$$

where μ is the displacement ductility ratio, Δu is the ultimate displacement, and Δy is the yield displacement. Yield displacement and yield base shear are judged through an idealization of the capacity curve. Ductility reduction factor $R\mu$ is a function of structural characteristics such as ductility, damping, and fundamental period of vibration (T), and the characteristics of earthquake ground motion. In this study, the formulation proposed by Newmark & Hall (1982) [39] is used:

$$R\mu = \sqrt{(2\mu - 1)} + 2(T - 0.5) \times \left(\mu - \sqrt{(2\mu - 1)}\right) \tag{4}$$

where $R\mu$ is the ductility reduction factor and μ is the displacement ductility.

The target displacement is calculated from the idealized pushover curve, idealization of the pushover curve can be done using the FEMA [34] coefficient method through the following relation:

$$\Delta u = \delta_t = C_0 C_1 C_2 C_3 S_a \frac{Te^2}{4\pi^2} g \tag{5}$$

where C_0 is modification factor to relate spectral displacement of an equivalent SDOF system to the roof displacement of the building MDOF system, C_1 is modification factor to relate expected maximum inelastic displacements to displacements calculated for a linear elastic response, C_2 is modification factor to represent the effect of pinched hysteretic shape, stiffness degradation, and strength deterioration on maximum displacement response, C_3 is modification factor to represent increased displacements due to dynamic $P - \Delta$ effects, S_a is response spectrum acceleration, at the effective fundamental period and damping ratio of the building in the direction under consideration, g is acceleration of gravity, and T_e is the effective fundamental period of the building in the direction under consideration in seconds.

4.3. Provisions of 'R' Factor in International Codes and Guidelines

Depending on the type of structural system and ductility class of the structures, the R-factor in different codes and recommendations varies. For Shear wall-frame, values of "R" as specified in IBC2018, ASCE [40-42], Eurocode-8 [29], and ECP 2012 [2] are presented in Table 2.

Table 2. R values are allocated in different codes for concrete shear wall-frame structures

Structural System		R-Value		
		IBC2018 ASCE7-16	Eurocode-8	ECP 2012
Frame system, dual system, coupled wall system	Medium ductility class (DCM)		3.0 Vu /Vy	
	High ductility class (DCH)		4.5 Vu /Vy	
Dual system from Moment Resisting Frames and Shear Walls	Limited ductility frame			5.0
	Sufficient ductility frame			6.0
Shear wall-frame interactive system with ordinary reinforced concrete moment frame and ordinary reinforced concrete shear walls		4.5		

For multi-bay multi-story $Vu/Vy = 1.3$, and for single-bay multi-story $Vu/Vy = 1.2$.

5. Nonlinear Static Analysis (Pushover Analysis)

The current work applies nonlinear static analysis (pushover analysis) to determine the global limit states of the RC moment-resistant frame in terms of drift and force level. The increasing forcing function is imposed on a mathematical model of a building, either in terms of horizontal forces (representation of inertial forces along the structure height) or displacements. When the target displacement or final limit state is attained, the analysis is finished [43]. This type of study can determine the building's maximal strength and deformation capacity. They also help identify possible weak and soft stories within the framework. Nonlinear static analysis is used to find the global limit states with the loading profile of the first mode shape. The mode shapes, period of structure in each mode, and modal participation factor are evaluated using modal or Eigenvalue analyses. This simple analysis is useful as an initial validation tool of the analytical models.

6. Finite Element Modeling

Exact modelling of the nonlinear behaviour of RC shear walls, which are the primary lateral-force-resistant structural members in high-rise buildings, is a critical task. As the cross-section of the shear wall member is much bigger than that of the beam and column member, its deformation behavior under the lateral load is more complicated [44]. So, it's very important to focus on the nonlinear analysis model for the shear wall.

6.1. Performance-Based Design Methodology

Structures with predictable performance within predetermined levels of risk and dependability are the result of performance-based engineering [34, 45]. The main goal is to keep the structure from collapsing completely. This indicates that the top-level can sustain a catastrophic collapse (CP); the sub-level, which houses the critical structures, can be minimally damaged yet still be occupied immediately (IO). There is a life safety (LS) level condition between the sub and higher levels. The nonlinear load-deformation relation must be defined according to FEMA's nonlinear procedures. Figure 8 depicts such a curve.

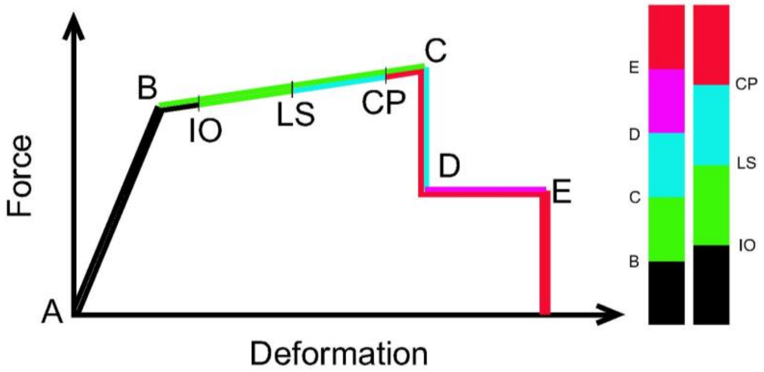

Figure 8. Typical load-deformation relation and target performance levels (ETABS)

According to FEMA, the five points (A, B, C, D, and E) are utilized to characterize the hinge rotation behaviour of RC components. The hinge's approval standards are defined by three additional points: immediate occupancy (IO), life safety (LS), and collapse prevention (CP). ASCE (2017b) [46] provides the illustrated damage for concrete frames at various structural performance levels in Table 3.

Table 3. Damage for concrete frames at different levels (ASCE, 2017b)

Elements	Immediate Occupancy (IO)	Life Safety (LS)	Collapse Prevention (CP)
Primary Elements	Minor cracking, limited yielding possible at a few locations. Minor spalling of concrete cover.	Extensive damage to beams. Spalling of cover and shear cracking in ductile columns. Minor spalling in non-ductile columns. Joint cracks.	Extensive cracking and hinge formation in ductile elements. Limited cracking or splice failure in some non-ductile columns. Severe damage in short columns.
Secondary Elements	Minor spalling in a few places in ductile columns and beams. Flexural cracking in beams and columns. Shear cracking in joints.	Major cracking and hinge formation in ductile elements. Limited cracking or splice failure in some non-ductile columns. Severe damage in short columns.	Extensive spalling in columns and beams. Limited column shortening. Severe joint damage. Some reinforcing buckled.
Drift	Transient drift that causes minor or no non-structural damage. Negligible permanent drift.	Transient drift is sufficient to cause nonstructural damage. Noticeable, permanent drift.	Transient drift is sufficient to cause extensive non-structural damage. Extensive permanent drift.

6.2. Layer Shell Modeling

The multi-layer shell element is based on composite material mechanics concepts and can model RC shear walls linked in-plane/out-plane bending and coupled in-plane bending-shear nonlinear behaviours. Figure 9 shows the basic concepts of a multi-layer shell element. The shell element is made up of several layers of varying thicknesses. Various material characteristics are ascribed to different layers. This indicates that the rebar has been spread into one or more layers. During the finite element computation, the axial strain and curvature of the intermediate layer may be calculated in one element. Using the assumption that the plane stays flat, the stresses and curvatures of the other layers may then be calculated. The corresponding stress will then be calculated using the constitutive relations of the material assigned to the layer.

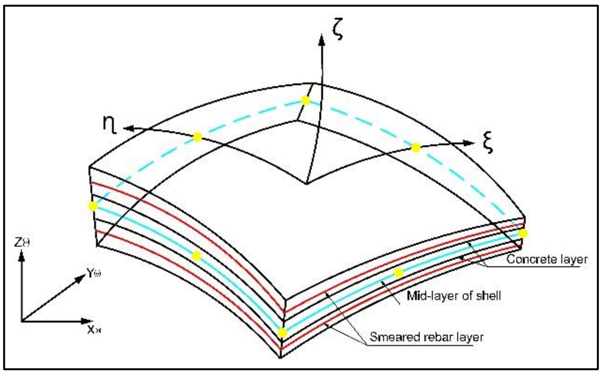

Figure 9. Basic concepts of the multi-layer shell element

The constitutive model of the rebars is given as a perfect elasto-plastic model. Because the rebars in various directions are smeared into one layer, the rebar layer may be set as isotropic if the longitudinal and transverse ratios of the distributing rebars to the concrete are the same. However, if the ratios in the two directions differ, the rebar layer should be orthotropic, with two primary axes, as illustrated in Figure 10.

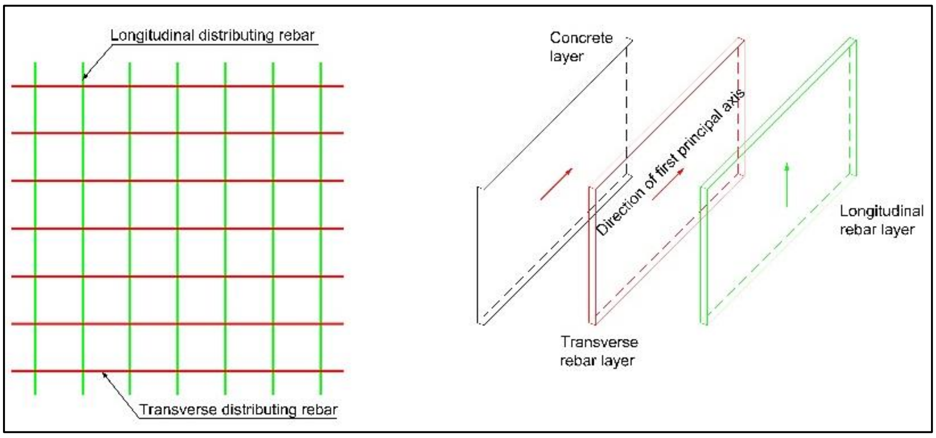

Figure 10. Settings of the rebar layers in multi-layer shell element

6.3. Fiber Shell Modeling

The 3D interaction (yield) surface of P-M2-M3 hinges may be defined explicitly, or automatically through AISC-LRFD eqn. H1-1a and H1-1b (Φ=1) FEMA-356 "Equations 4 and 5" for steel, or ACI 318-02 [47] (Φ=1) for concrete. The post-yield behaviour is interpolated from one or more user-defined P- curves, where M2 and M3 are represented by the relationship. During analysis, an energy-equivalent moment-rotation curve is generated during analysis in relation to the input P-curve(s) and the interaction-surface yield point.

The moment-rotation curve of a P-M2-M3 hinge, which is a monotonic backbone relationship, describes the post-yield behaviour of a beam-column element exposed to combined axial and biaxial-bending conditions. The 3D interaction surface of a P-M2-M3 hinge indicates the envelope of yield points. Performance must be extrapolated from one or more moment-rotation curves beyond this point. Because the P-M2-M3 response in three dimensions extends linearly to the yield surface. Figure 11 shows the shell element model for the walls, while Figure 12 shows the moment and rotation values of a P-M2-M3 moment-rotation curve, which could be obtained through basic geometric relationships between components projected along the M2 and M3 axes.

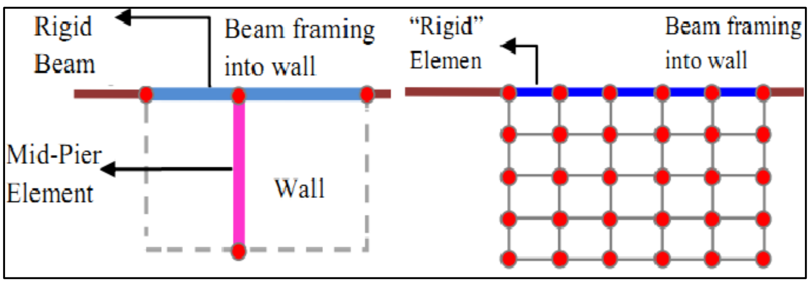

Figure 11. Shell element model for the shear wall

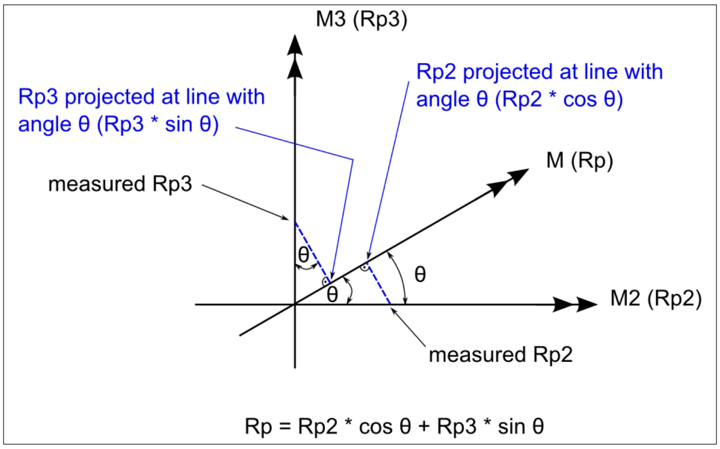

Figure 12. Moment and rotation components

Hinge's reinforcement could be assigned in different ways from the design, uniform ratio, and as a specified layout, which had been used in the current study. Figure 13 shows the analysis flow chart.

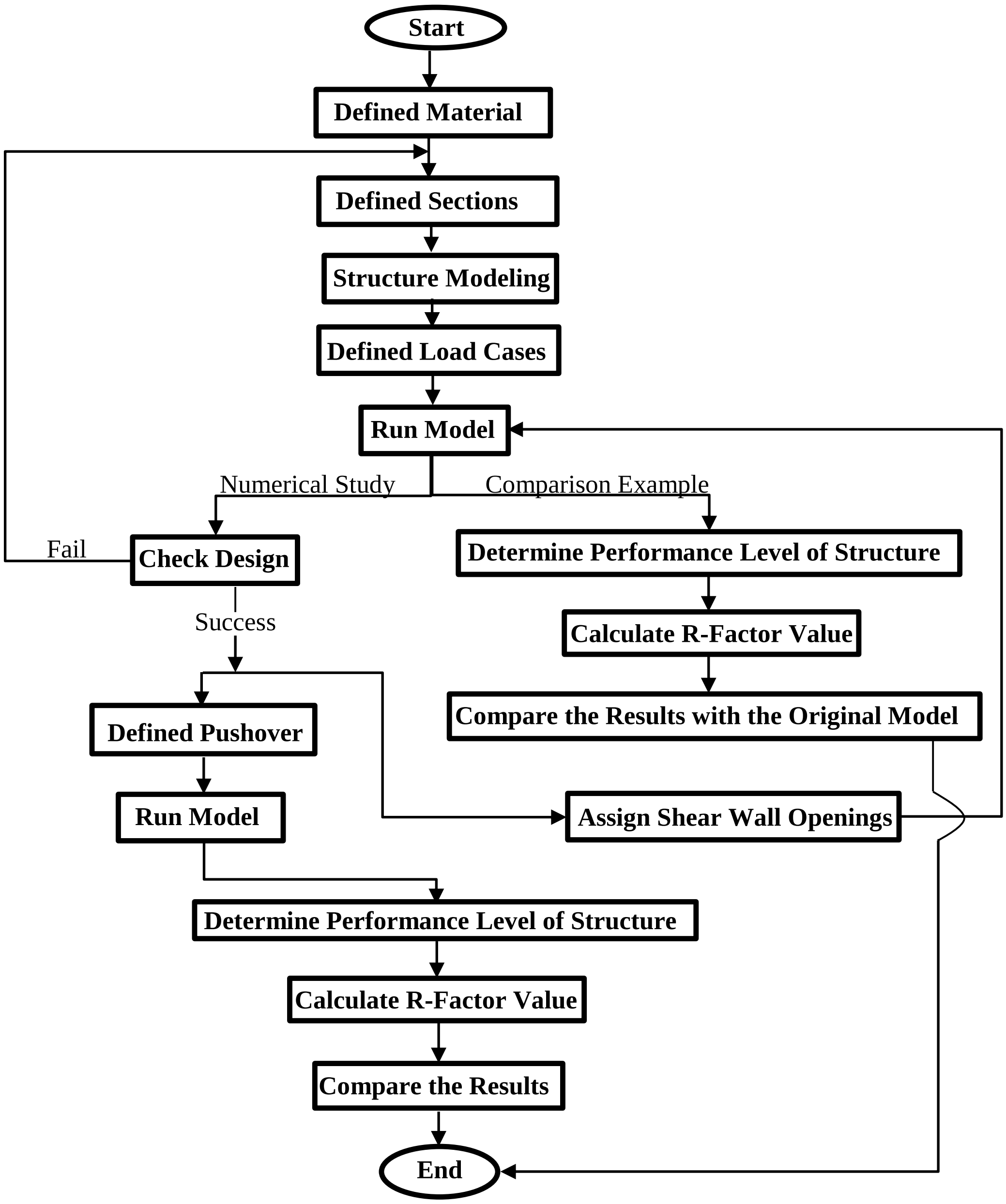

Figure 13. Analysis Flow Chart

7. Comparison Example

A study was conducted for an 8-story Dual System building, which was studied by Yasser, I., et al. [5] and modelled using both SAP 2000 [4] and ETABS [3] software.

7.1. Models Description

Eight-stories Dual-system buildings have five bays in both directions. The storey height is 3.2 m, and the total width of the building is 26.3 m. The building plan and 3D view are presented in Figure 14. Material stress-strain curves for concrete and steel are shown in Figure 15. Two different modelling methods (fiber and layered) are used to model the shear walls. Performance based design is carried out on the buildings using nonlinear static pushover analysis as per ATC-40 and FEMA 356. Plastic hinges are allocated at the locations where yielding is predicted under seismic forces at both ends of the beams and columns, with start and end relative distances of 0.05 and 0.95, respectively. In the fiber model, hinges are also given to the walls. As per ASCE 41-13 [40], the plastic hinge type allocated to columns is interacting (P-M2-M3), while the type assigned to beams is M3, which is a single moment rotation type. In the fiber model, the walls are (P-M3). With a zero initial condition and a nonlinear static gravity load case containing their own weight multiplied by a scale factor of (1), super dead load multiplied by a scale factor of (1), and a live load multiplied by a scale factor of (0.25), the mass source is (Dead Load + Super Dead Load + 0.25 Live Load). Nonlinear static pushover load cases in global X-Direction with a static lateral load pattern are applied to the structure starting from the end of the nonlinear gravity load case with a target displacement equal to 4% of the total building height.

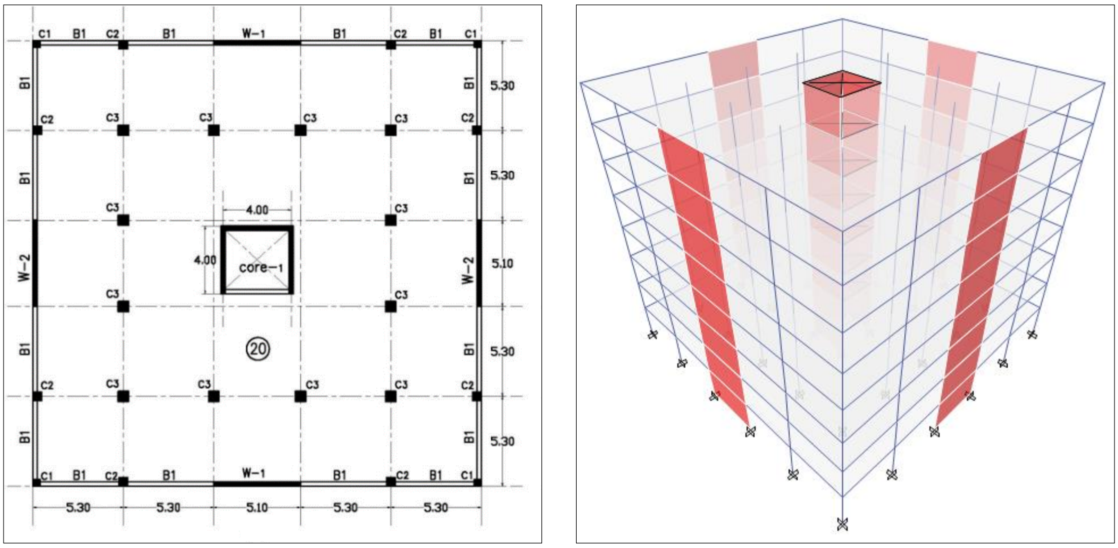

(a) Building plan view (b) Building 3D-view

Figure 14. Building Configuration

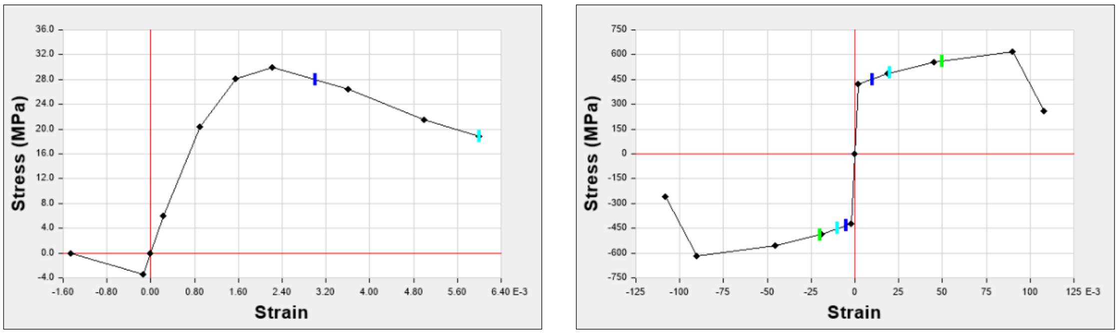

Figure 15. Stress-strain curve for concrete and rebar material

7.2. Results and Discussion

Figure 16, and Table 4 present the results for ETABS 2016 Layered shell and Fiber models, and the Layered shell SAP2000 model Compared with the original paper Layered shell SAP2000 model:

- The internal stress, hinge formation, and wall displacement for fiber and layered shell models are shown in Figure 16. Internal stresses were easily noticeable in the layered shell model, while the fiber model allowed for the observation of hinge formation in walls, and both models could display displacement.

- The fiber model pushover curve has been compared with the present study's layered shell SAP2000 and ETABS model curves, and with the curve mentioned in the original paper as shown in Figure 17. Which shows a slight difference between the curves within an acceptable limit. Using a shear wall fiber model is perfect. It enables us to observe the performance levels of the shear wall under lateral loads and determine the base shear and top displacement for each level.
- The comparative verification results showed that the values of the R factor obtained from static nonlinear analysis by SAP2000 for the original paper and verified models by SAP2000 and ETABS varied from 0.5 to 7.0%, as shown in Table 4 which is acceptable. The value of the R-factor obtained by ETABS 2016 for both the fiber and layered shell models is almost the same.
- ETABS 2016 v16.2.1 gives accurate results similar to other authors' experimental and other software results and could be reasonable for our study. Also, using the shear wall fiber model is perfectible, it enables to observe the performance levels for the shear wall under lateral loads and determine the base shear and top displacement for each level.

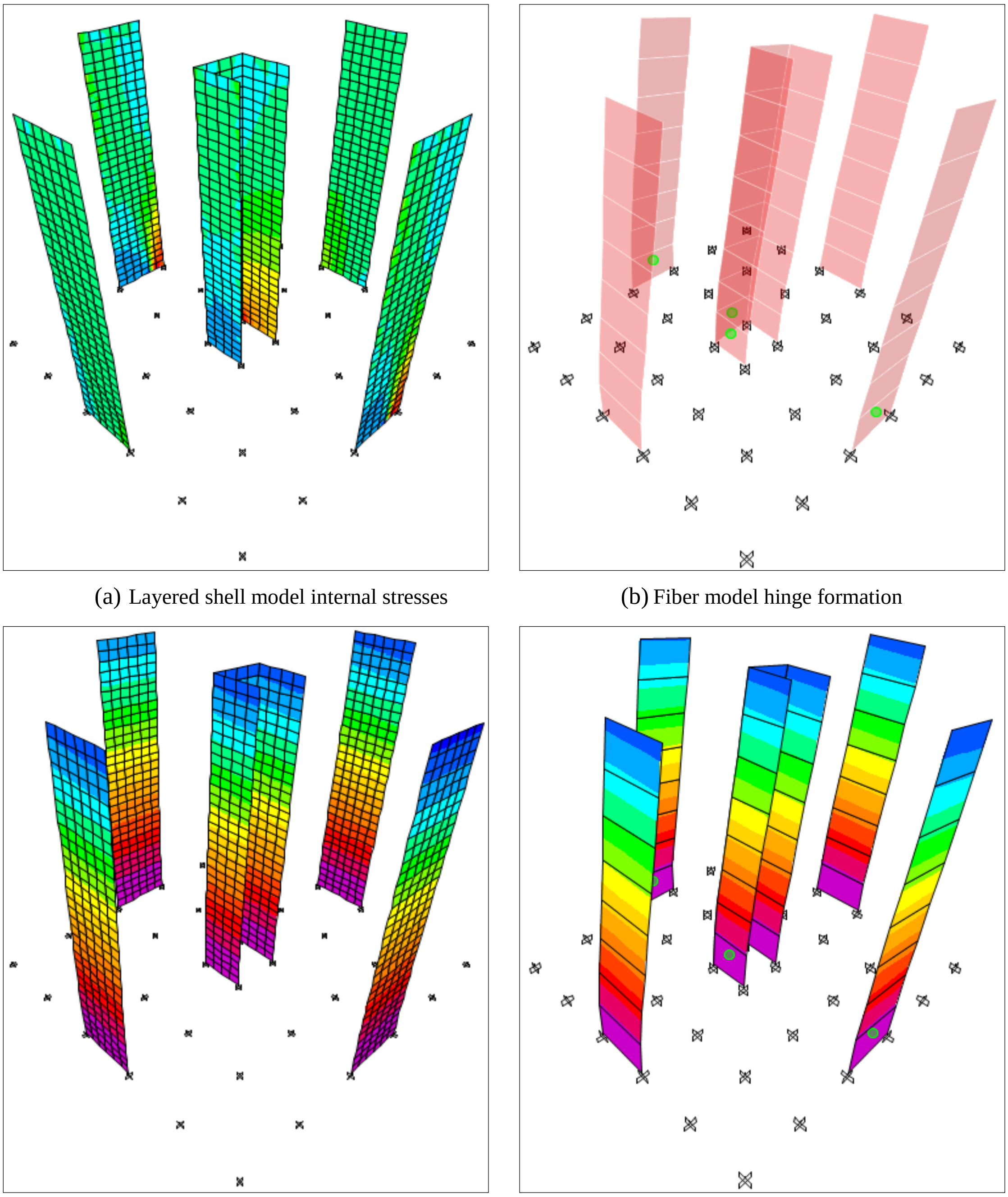

(a) Layered shell model internal stresses (b) Fiber model hinge formation

(c) Layered shell model displacement (d) Fiber model displacement

Figure 16. Fiber and Layered Shell Internal Stress, Hinges Formation, and Walls Displacement

Table 4. Comparison between Present Study R-Values and the Value obtained by Yasser et al. (2018)

Model	Software	R-Factor
Yasser et al. (2018) [5]	SAP2000	5.53
Layered shell Model	SAP2000	5.14
Layered shell Model	ETABS 2016	5.50
Fiber Model	ETABS 2016	5.60

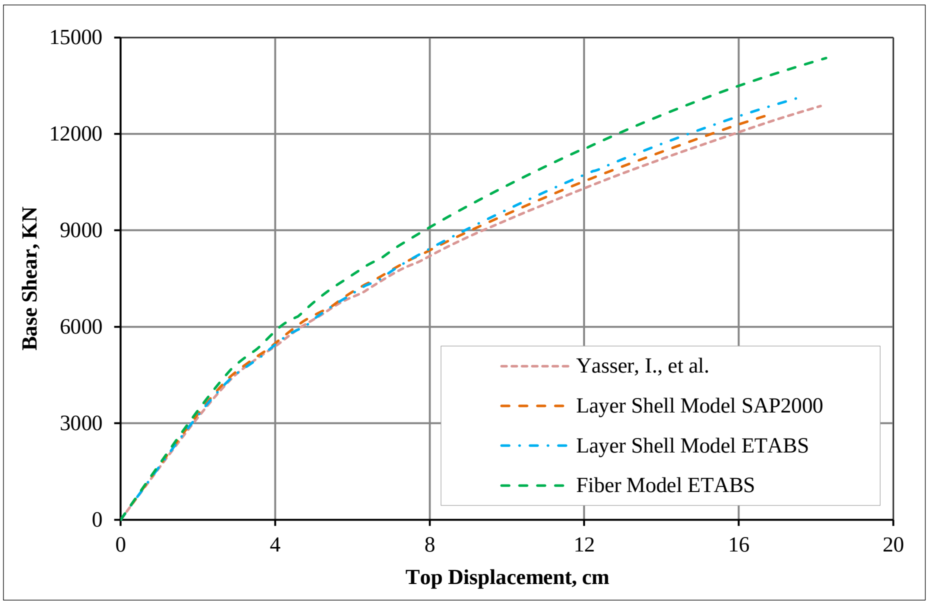

Figure 17. Comparison between the Present Study Fiber and Shell Models Pushover Curves and the Curve Obtained by Yasser et al. (2018)

8. Numerical Study for Seismic Response Modification Factor for Shear Wall without Openings in Multi-Storey Dual System Buildings

Sixteen and eight-stories reinforced concrete buildings have 5 bays for both X and Y directions, with a 26.3×26.3 m^2 and a storey height of 3.2 m, which are 52.2 and 25.6 m tall, respectively. Material properties and stress-strain curves for concrete and steel are illustrated in Table 5 and Figure 18 respectively. The plan, 3D-View, is shown in Figure 19.

Table 5. Material properties for models

F'c	30 MPa	Concrete strength
Fy	420 MPa	Rebar yield strength
Ec	24100 MPa	Modulus of elasticity of concrete
Es	200000 MPa	Modulus of elasticity of Rebar
G	10041.58 MPa	Shear modulus
Y	0.2	Poisson's ratio

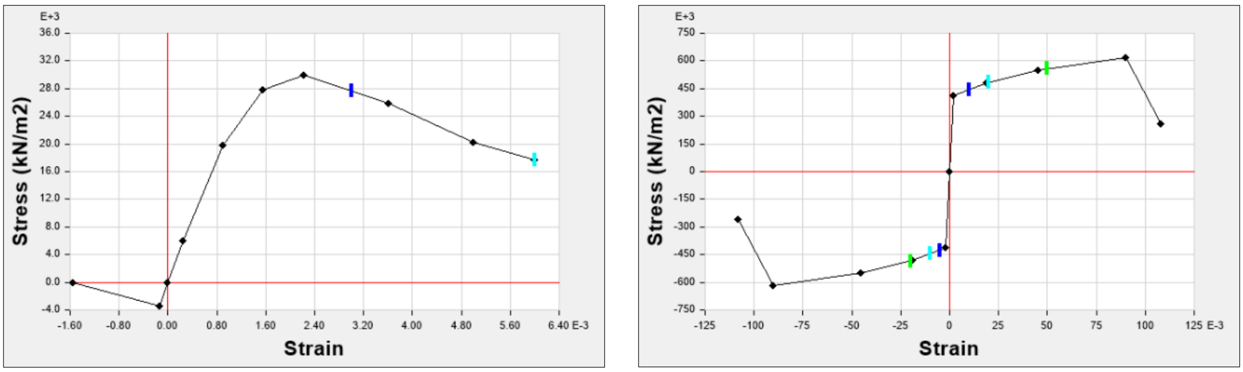

Figure 18. Stress-strain curve for concrete and rebar material

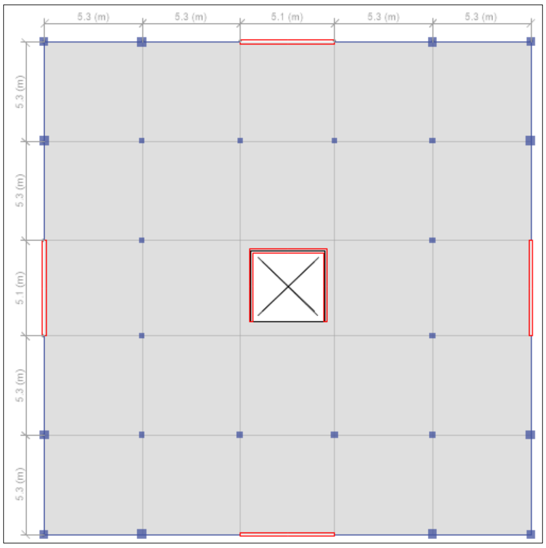

Model Plan (A) Sixteen Stories

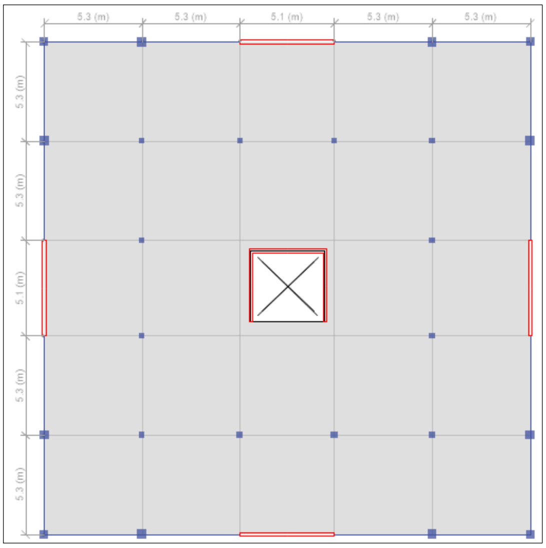

Model Plan (B) Eight Stories

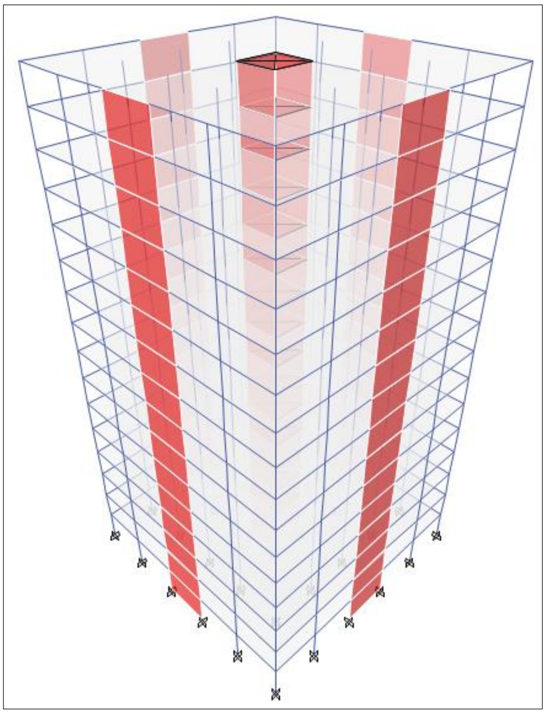

Model 3D-View (A) Sixteen Stories

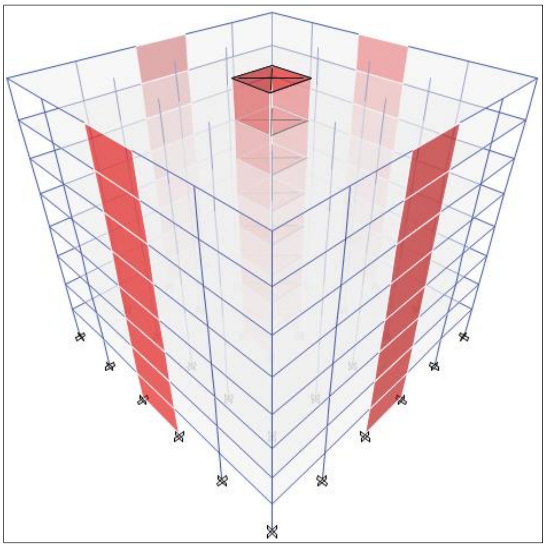

Model 3D-View (B) Eight Stories

Figure 19. The layout of studied buildings Models

The seismic load-bearing system consists of dual-system shear walls and frames, while the gravity load-bearing solution is built up of a 200-mm-thick concrete flat slab supported by reinforced concrete columns and shear walls. In both X and Y orientations, shear walls and core thicknesses equal 400, 300, and 200 mm for the first five stories, the second five stories, and the last six stories, respectively, 350, 250, and 200 mm for the first five stories, the second five stories, and the last six stories, respectively, in model type (A). While shear walls and core thicknesses in both X and Y directions in model type (B) are 350 and 300 mm in the lower four stories, respectively, and 300 and 250 mm in the upper four stories, as shown in Tables 6 and 7.

Table 6. Designed sections for type (A) 16-story

Columns Sections		
Column ID	**Cross-sec (mm×mm)**	**Main bars**
C1 (1-4)	1350×1350	40T32
C1 (5-8)	1000×1000	20T28
C1 (9-12)	750×750	12T25

C1 (12-16)	550×550	12T20
C2 (1-8)	850×850	32T20
C2 (9-16)	800×800	28T20
C3 (1-5)	800×800	28T20
C3 (6-10)	650×650	16T20
C3 (11-13)	500×500	16T16
C3 (14-16)	350×350	8T16
Beams Sections		
Beam ID	**Cross-sec (mm×mm)**	**Reinforcement at supports**
		Upper & lower
B1	250×850	12T22
Walls Sections		
Wall ID	**Thickness(mm)**	**Shear wall sections and Reinforcement**
		VL RFT / HL RFT
Core (1-5)	350	T20@125 / T12@200
Core (6-10)	250	T16@200 / T12@200
Core (11-16)	200	T12@200 / T12@200
W (1-5)	400	T20@100 / T12@200
W (6-10)	300	T20@200 / T12@200
W (11-16)	200	T12@165 / T12@200

Table 7. Designed sections for type (B) 8-story

Columns Sections		
Column ID	**Cross-sec (mm×mm)**	**Main bars**
C1 (1-2)	800×800	28T20
C1 (3-4)	700×700	24T18
C1 (5-6)	650×650	20T18
C1 (7-8)	600×600	20T16
C2	750×750	24T20
C3 (1-2)	600×600	20T16
C3 (3-4)	500×500	16T16
C3 (5-6)	400×400	12T14
C3 (7-8)	300×300	8T14
Beams Sections		
Beam ID	**Cross-sec (mm×mm)**	**Reinforcement at supports**
		Upper & lower
B1	250×1150	19T16
Walls Sections		
Wall ID	**Thickness(mm)**	**Shear wall sections and Reinforcement**
		VL RFT / HL RFT
Core (1-4)	300	T20@200 / T12@200
Core (5-8)	250	T16@200 / T12@200
W (1-4)	350	T20@150 / T12@200
W (5-8)	300	T18@200 / T12@200

8.1. Models Description

The two models have been well designed according to the Egyptian code and checked according to the European code, taking into consideration the previous mentioned considerations. Columns' P-M-M interaction ratios and wall D/C ratios should be less than one to ensure safety and compliance with Egyptian standards and the European code. Performance based design is performed on the two models as per ASCE 41-13 [40] before conducting openings using nonlinear static pushover-analysis. Seismic load is defined as per the Egyptian standards and Euro code. The following loading assumptions were taken into account:

Total Dead Load (D) is equal to DL+SDL+CL;

- Dead Load (DL) is equal to the self-weight of the members;
- Super-imposed Dead Load (SDL) equals 1.5 kN/m². SDL does not include partitions weight;
- Live Load (L) equals 2.0 kN/m².

According to ECP 2012, the structures under investigation are subjected to various load combinations. The following terms are used to describe these combinations:

$$U = 1.40\,D + 1.60\,L \tag{6}$$

$$U = 1.12\,D + \alpha\,L \pm S \tag{7}$$

where D is the dead load, L is the live load; S is the seismic load and superposition factor of the structure's the residential buildings. With a zero initial condition and a nonlinear static gravity load case containing their own weight multiplied by a scale factor of (1), super dead load multiplied by a scale factor of (1), and a live load multiplied by a scale factor of (0.25), the mass source is (Dead Load + Super Dead Load + 0.25 Live Load).

Nonlinear static pushover load cases in global X-Direction with static lateral load pattern are applied to the structure starting from the end of the nonlinear gravity load. While the target displacement equals 4% of the total building height. Plastic hinges are assigned at the locations where yielding is expected under seismic forces at both ends of the beams and columns, with start and end relative distances of 0.05 and 0.95, respectively. Also, hinges are assigned to walls. As per ASCE 41-13 [40], the plastic hinge types assigned to columns, beams, and walls are interacting (P-M2-M3), single moment rotation type (M3), and (P-M3) respectively.

8.2. Results and Discussion

After completing the design and allocating the hinges, a pushover nonlinear analysis was performed to evaluate the yield and ultimate forces and displacement. After drawing the pushover curve, the ultimate and yield steps were established using Acceptance Criteria Limits for Hinges Deformation, Park Definition [36] for Ultimate and Yield Deformation, and ASCE 41-13 [40] Idealized Bilinear Curve. The R-values determined using the previously discussed approaches are shown in Tables 8 to 10.

- The values produced by the three approaches differ by a minor amount, indicating that any of them may be used to determine the R-factor.
- The R-factor for the 16-story model ranges from 4.01 to 4.94, while the R-factor for the 8-story model ranges from 5.56 to 5.85, depending on the followed method of calculation.
- Calculated R-factor values comply with the given value of R-factor Eurocode-8 (2012) for dual-system models.

Table 8. Acceptance Criteria Limits for Hinges Deformation Results

Model	Time Period	Δu	Δy	μ	Rμ	Vy	Vd	Vu	Rs	R
	(sec)	m	m			kN	kN	kN		
1-A (16-Story)	1.656	0.620	0.277	2.24	2.24	25459.83	11533.00	36713.35	2.21	4.94
1-B (8-Story)	0.632	0.243	0.104	2.33	2.03	25957.97	9467.39	33737.89	2.74	5.56

Table 9. Park Definition [42] for Ultimate and Yield Deformation Results

Model	Time Period	Δu	Δy	μ	Rμ	Vy	Vd	Vu	Rs	R
	(sec)	m	m			kN	kN	kN		
1-A (16-Story)	1.656	0.87	0.54	1.60	1.60	34768.90	11533.00	41149.15	3.01	4.83
1-B (8-Story)	0.632	0.32	0.16	1.95	1.77	30290.81	9467.39	36159.32	3.20	5.66

Table 10. ASCE 41-13 Idealized Bilinear Curve Results

Model	Time Period	Δu	Δy	μ	Rμ	Vy	Vd	Vu	Rs	R
	(sec)	m	m			kN	kN	kN		
1-A (16-Story)	1.656	0.42	0.19	2.17	2.17	21315.91	11533.00	31171.62	1.85	4.01
1-B (8-Story)	0.632	0.19	0.06	3.03	2.45	22571.17	9467.39	31404.12	2.38	5.85

Figure 20 presents the relationship between the R-factor values calculated by three different methods.

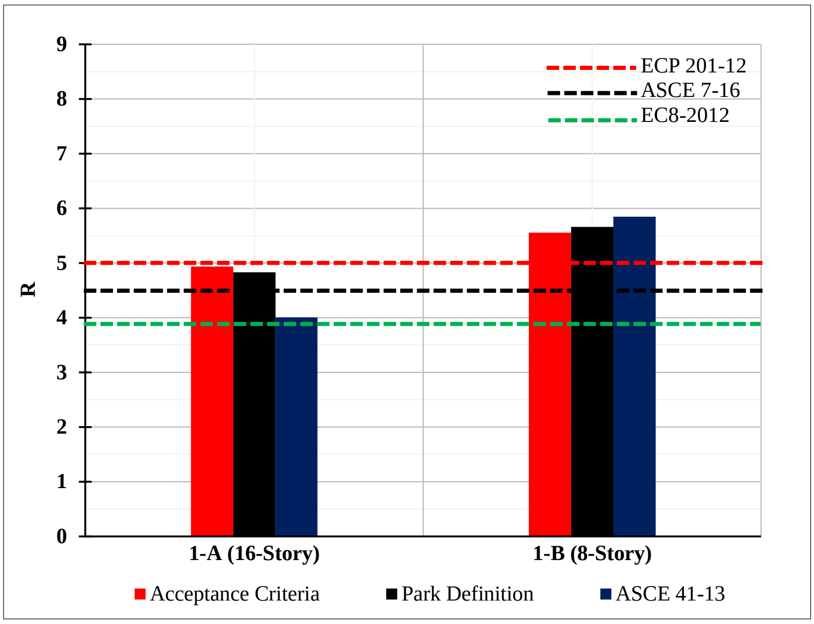

Figure 20. Comparison between R-Factor calculated using different techniques and the value obtained by ECP 201-12, ASCE 7-16, and EC8-2012

9. Numerical Study for Seismic Response Modification Factor for Shear Wall with Openings in Multi-Storey Frame Buildings

Using openings of various sizes, defining the lintel beam as a spandrel, wall segment, and adding additional steel surrounding openings, numerical research was carried out on previously designed structures. Acceptance criteria limits for the hinge deformation technique used to calculate the R-Factor.

9.1. Models Description

1.8×1.8, 2.75×1.8, and 1.8×2.75 openings have been applied to the outer shear walls of the two previously designed buildings. Figures 21 and 22 present the 3-D views of sixteen and eight-story models after applying the opening, respectively.

Lintel beam can be defined into two different methods, first, by defining lintel as a wall segment. Second, by defining it as a spandrel. Table 11 presents the model symbols, a number of stories, ground acceleration, spectrum type, and the dimension of openings applied.

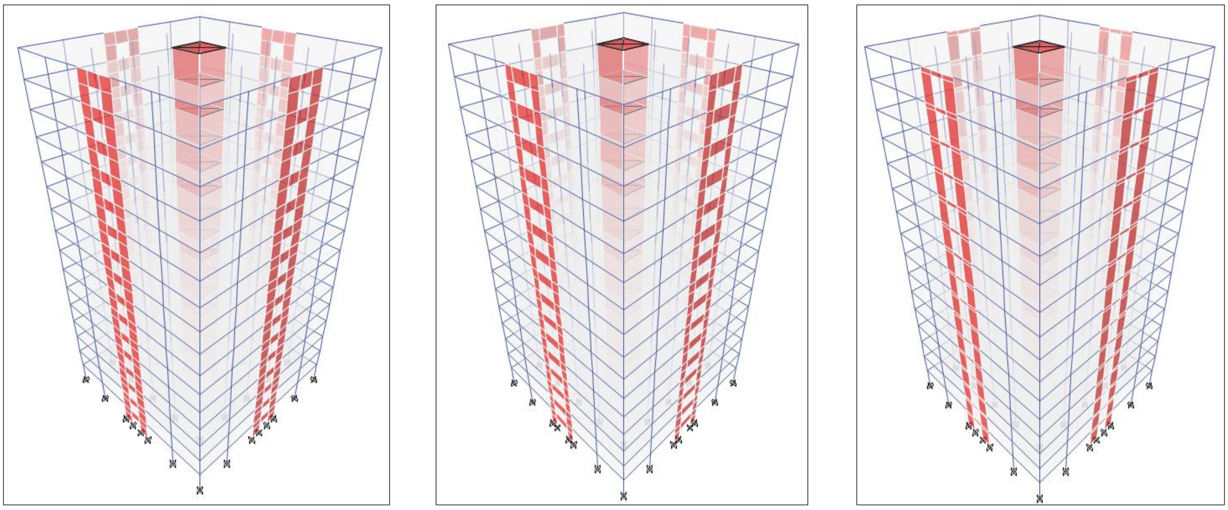

(a) Model with Opening 1.80 Width and 1.80 Height, (20% opening)

(b) Model with Opening 2.75 Width and 1.80 Height, (30% opening)

(c) Model with Opening 1.80 Width and 2.75 Height, (30% opening)

Figure 21. Model type (A), (B) 16-Story 3D-View

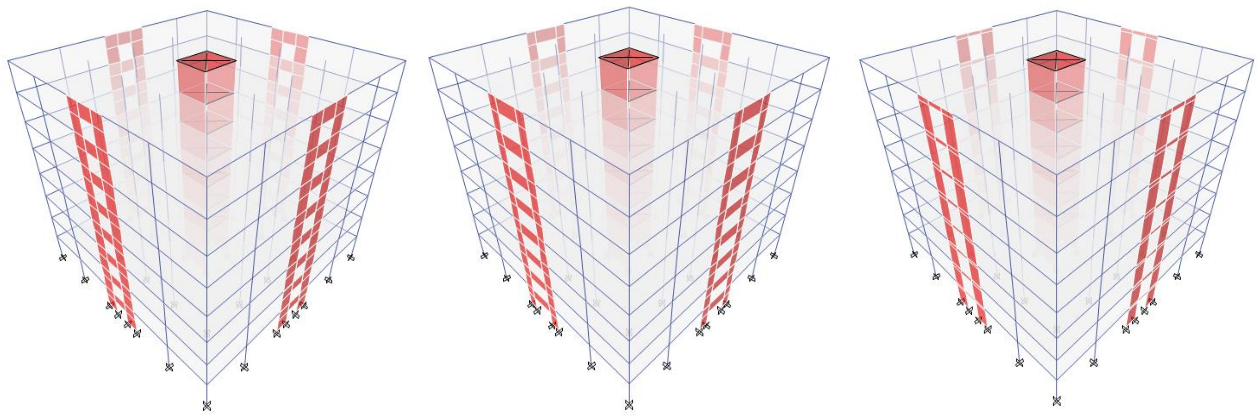

(a) Model with Opening 1.80 Width and 1.80 Height, (20% opening) (b) Model with Opening 2.75 Width and 1.80 Height, (30% opening) (c) Model with Opening 1.80 Width and 2.75, (30% opening)

Figure 22. Model type (A), (B) 8-Story 3D-View

Table 11. Numerical and Their Range (Lintel beam defined as a wall Segment)

Model	No. of Stories	Ground Acceleration (ag/g)	Spectrum Type	Opening Dimension		
				B (m)	×	H (m)
1-A	16	0.25	1	-	×	-
2-A				1.80	×	1.80
3-A				2.75	×	1.80
4-A				1.80	×	2.75
1-B	8	0.25	1	-	×	-
2-B				1.80	×	1.80
3-B				2.75	×	1.80
4-B				1.80	×	2.75

9.2. Results and Discussion

After pushover analysis, a series of pushover curves have been plotted, which are used to calculate the R-factor parameters (ultimate displacement, yield displacement, and yield base shear) and evaluate the (R) factor. Figures 23 and 24 present the base shear–displacement curves before and after the conduction of different sizes of openings for models of type (A), and (B) with 16, and 8 stories.

The previous figures show a small decrease in base shear due to the same displacement while the opening was conducted. By expanding the opening size, the decrease was enhanced. Table 12 shows the R-factor calculations utilizing the acceptance criteria limits for the hinges deformation method as well as identifying the lintel beam as a wall segment.

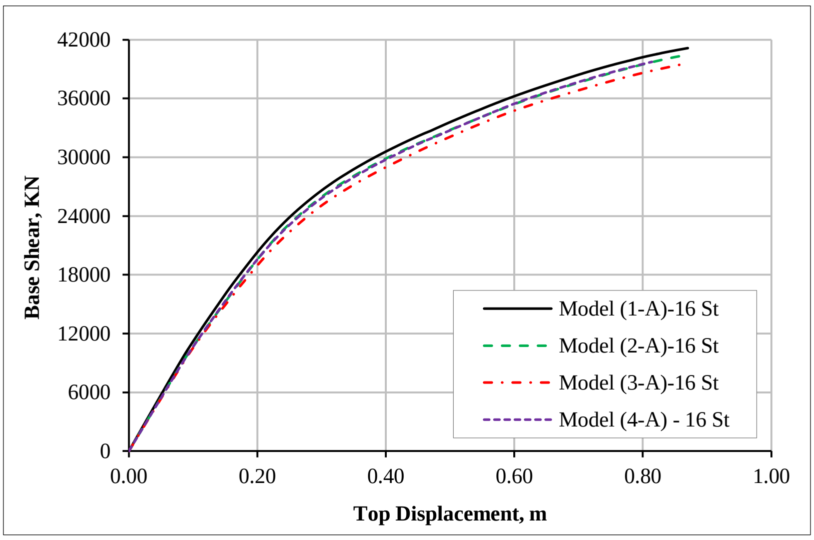

Figure 23. Models Type (A-16 story)

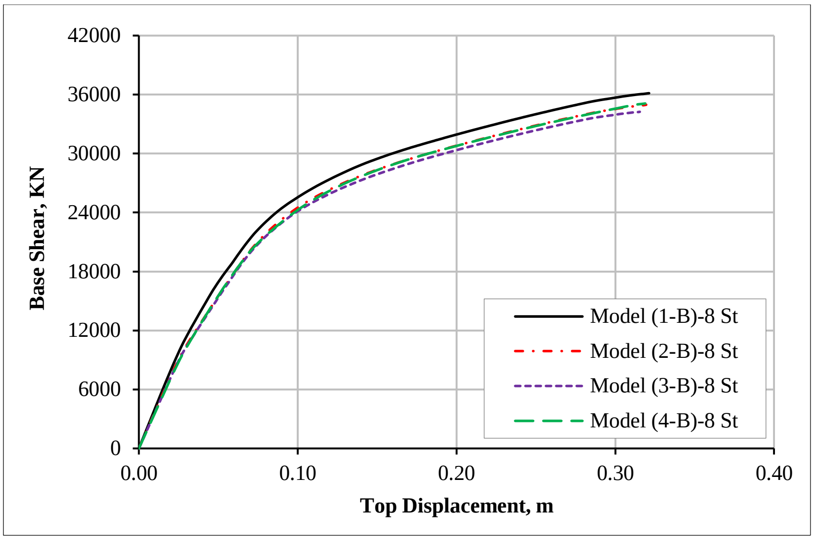

Figure 24. Models Type (B-8 story)

Table 12. Calculation of R according to Acceptance Criteria Limits for Hinges Deformation (Wall segment)

Model	Time Period	Δu	Δy	μ	Rμ	Vy	Vd	Vu	Rs	R
	(sec)	m	m			kN	kN	kN		
1-A (16-Story)	1.656	0.620	0.277	2.24	2.24	25459.83	11533.00	36713.35	2.21	4.94
2-A (16-Story)	1.695	0.655	0.368	1.78	1.78	28792.12	11427.00	36685.70	2.52	4.48
3-A (16-Story)	1.715	0.582	0.268	2.17	2.17	23399.00	11926.00	34318.71	1.96	4.26
4-A (16-Story)	1.702	0.582	0.354	1.64	1.64	28110.78	14369.00	34979.07	1.96	3.21
1-B (8-Story)	0.632	0.24	0.10	2.33	2.03	25957.97	9467.39	33737.89	2.74	5.56
2-B (8-Story)	0.659	0.24	0.11	2.14	1.92	25761.12	9373.14	32562.81	2.75	5.27
3-B (8-Story)	0.666	0.21	0.11	1.83	1.70	25333.94	9717.77	30659.16	2.61	4.43
4-B (8-Story)	0.675	0.22	0.13	1.63	1.55	27151.57	11534.00	31456.53	2.35	3.65

To increase the system's performance in the case of conducted openings, on either side of the openings, half of the reinforcing bars that were terminated to conduct openings have been added. Table 13 shows the results of two approaches for modelling the lintel beam above openings. The first is to regard the lintel beam as a wall piece (the openings have been conducted without changing the definition of the upper lintel). The second is to regard the lintel beam as a spandrel. Furthermore, the research was carried out using ground acceleration (ag/g) equal to 0.25, and a spectrum type (1).

Table 13. Response Reduction Factor (R) for Model A, and B (Different Modeling Methods)

Model	Response Reduction Factor (R)		
	Wall Segment	Spandrel	Additional Steel
1-A (16-Story)		4.94	
2-A (16-Story)	4.48	4.46	4.65
3-A (16-Story)	4.26	4.21	4.49
4-A (16-Story)	3.21	3.26	3.67
1-B (8-Story)		5.56	
2-B (8-Story)	5.27	5.19	5.42
3-B (8-Story)	4.43	4.45	4.59
4-B (8-Story)	3.65	3.65	3.96

Figures 25 to 29 indicates the relationship between the R-factor evaluated for both wall segment, spandrel modelling methods, and the improvement due to the additional steel laid beside the openings and value mentioned in the Egyptian code.

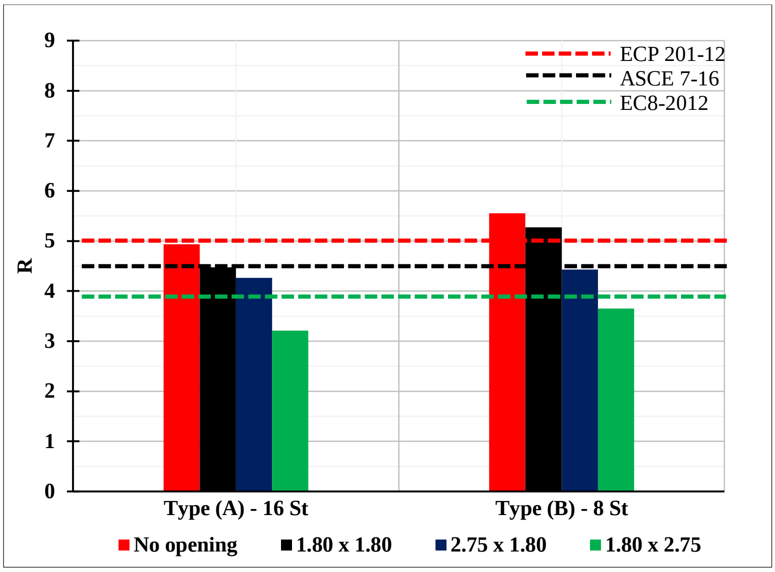

Figure 25. Relation between R and opening Dimension in different models (Wall Segment)

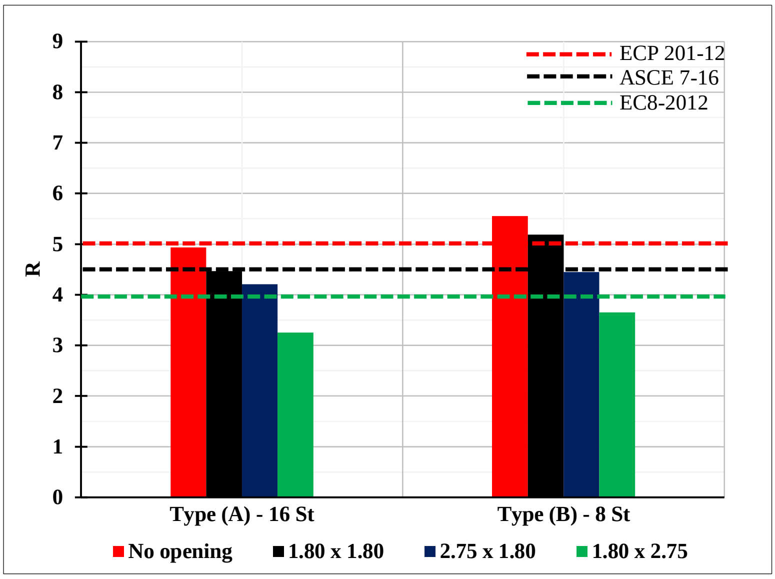

Figure 26. Relation between R and opening Dimension in different models (Spandrel)

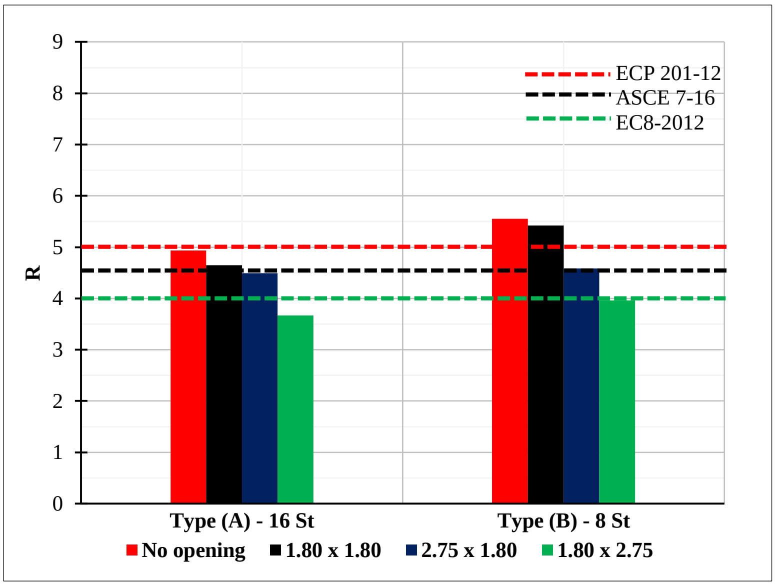

Figure 27. Relation between R and opening Dimension in different models (Additional Steel)

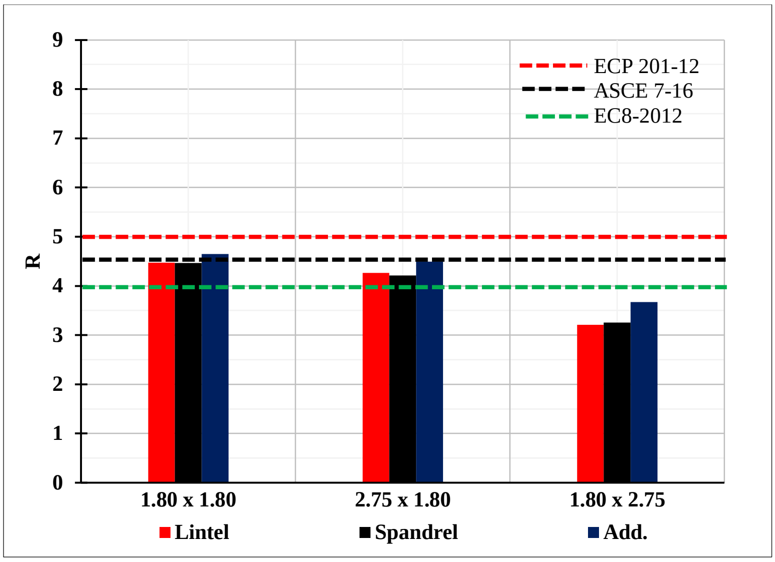

Figure 28. Models Type (A) 16-Story Additional Steel Improvement

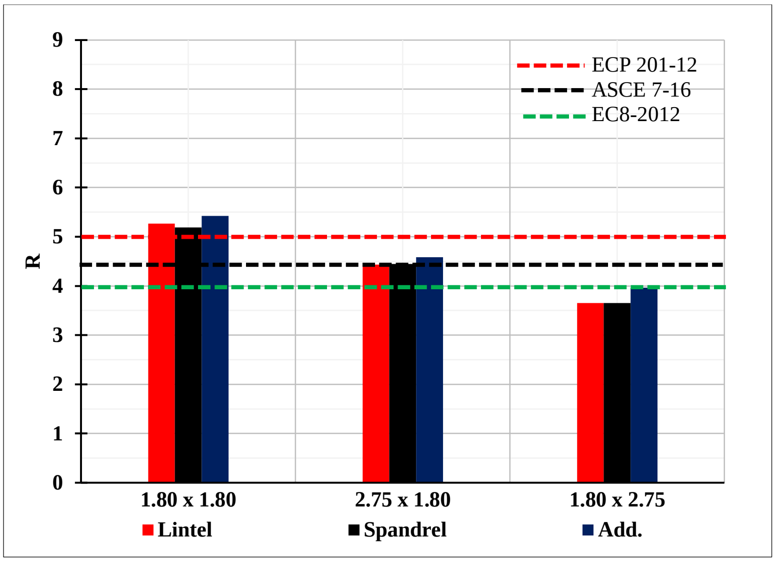

Figure 29. Models Type (B) 8-Story Additional Steel Improvement

Lintel Beam Defined as a Wall Segment

Figure 25 presents the relationship between the opening's dimension and the R-factor, clarifies the decrement in R-Factor due to the openings, and indicates that opening height is more critical than the width in the case of defining the lintel beam as a wall segment. As shown in Figure 25 above, it's obvious that by increasing the opening dimension, a reduction in the R-factor is observed. The influence of the opening height is more critical than the width.

Lintel Beam Defined as a Spandrel

Figure 26 presents the relationship between the opening's dimension and the R-factor, clarifies the decrement in R-Factor due to the openings, and indicates that opening height is more critical than the width in the case of defining the lintel beam as a spandrel. From Figure 26, modelling the lintel beam as a spandrel is better than modelling it as a wall segment as it is similar to its true behaviour and the result is almost the same in both methods. The spandrel gives flexibility in design and shows the bottom and upper main reinforcement by using the detailing tool.

The Influence of Adding Additional Steel around Openings

In an attempt to improve the performance of the shear wall, half of the reinforcement bars terminated to conduct openings have been added at both openings' sides. As shown in Figure 27, adding additional steel around the openings has an impact on the overstrength factor greater than the ductility factor. Figure 28, and Figure 29 indicate the relationship between the R-factor evaluated for both wall segment and spandrel modelling methods and the improvement due to the additional steel laid beside the openings. From the previous figures, it's clear that additional steel on either side of openings causes some improvement in R-factor, up to 12%.

Comparison between Results and the Factor Mentioned in Codes

For the limited ductility class of Dual Systems from Moment Resisting Frames and Shear Walls with an opening, the supplied value of R-factor = 5.0 at ECP-201 (2012) is an un-conservative number, as the accurate value of R-factor is smaller than the given value. For typical reinforced concrete moment frames, the American Society of Civil Engineers (ASCE7 -2016) and the International Building Code (IBC -2018) provide R-factors of 3.0.

The previous results indicate that:

- After conducting the openings, a small decrease in base shear due to the same displacement happened and the R-factor value decreased.
- The values of the R-factor increased by adding half of the rebars which had been terminated to conduct the openings.
- The R-factor is reduced by increasing the number of stories.
- The R-factor values after conducting openings decreased depending on the size and aspect ratio, as the opening height is more critical than the opening width for the same opening percentage.
- For the opening that represents 30% of the wall area, the R-factor for the height is 1.8 greater than the other opening with a height of 2.75 by 0.78 to 1.05 depending on the number of stories and the method of modeling.

10. Numerical Study for Seismic Response Modification Factor for Shear Wall with Ground Storey Openings in Multi-Storey Frame Buildings

A numerical study has been conducted on model types (A), and (B), which were previously designed by applying openings with dimensions of 2.75 m in height and 1.8 m in width only on the ground storey to obtain the ground storey openings impact. Acceptance criteria limits for the hinge deformation method used to evaluate the R-Factor.

10.1. Models Description

1.8×2.75 openings have been applied to the outer shear walls of the two previously designed buildings only on the ground floor. Figure 30 presents the 3-D views of the sixteen and eight-story models after applying the openings.

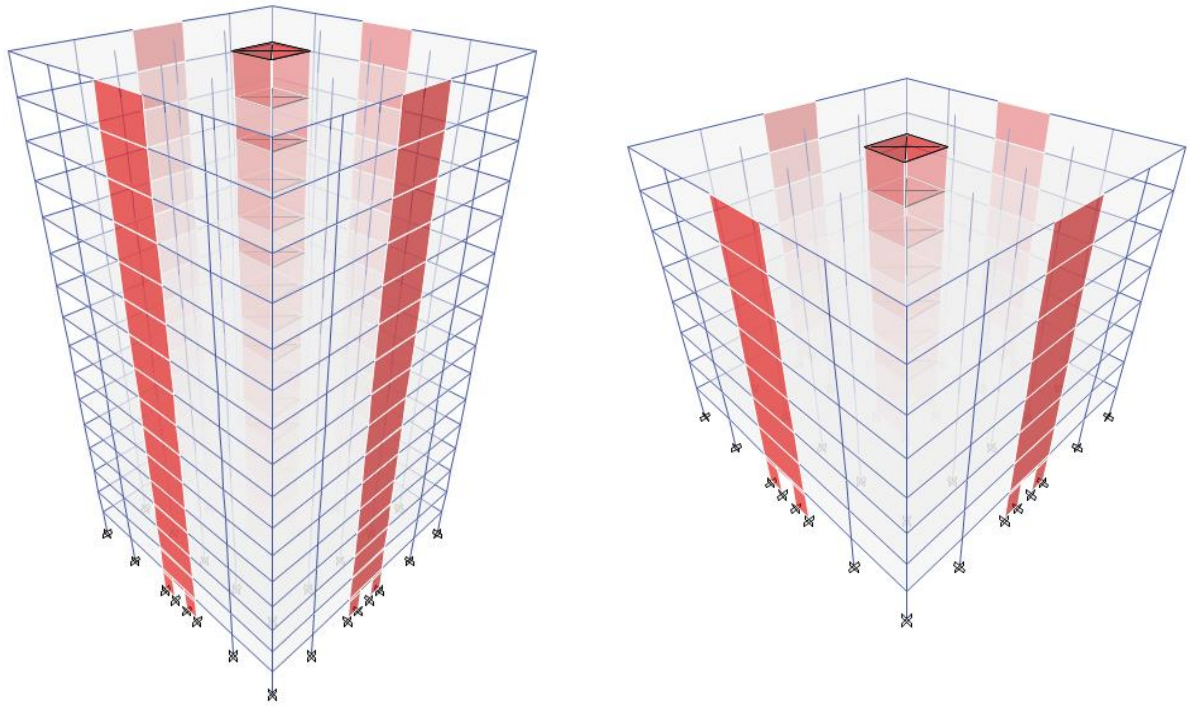

Model Type (A) 16-Storey with Ground Storey Opening 1.80 Width and 2.75 Height, (30% opening)

Model Type (B) 8-Storey with Ground Storey Opening 1.80 Width and 2.75 Height, (30% opening)

Figure 30. Model type (A), (B) 16-Storey and 8-Story 3D-View after Applying Ground Storey Openings

10.2. Results and Discussion

After pushover analysis, pushover curves have been plotted, which are used to calculate the R-factor parameters (ultimate displacement, yield displacement, and yield base shear) and evaluate the R-factor. Figures 31 and 32 present the base shear–displacement curves before and after conducting ground floor openings for types (A), and (B) models.

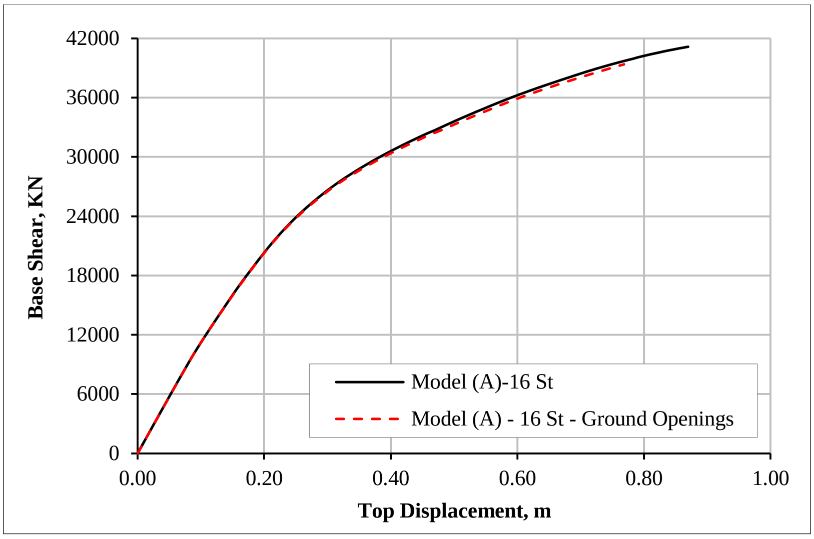

Figure 31. Models Type (A) - 16 Storey

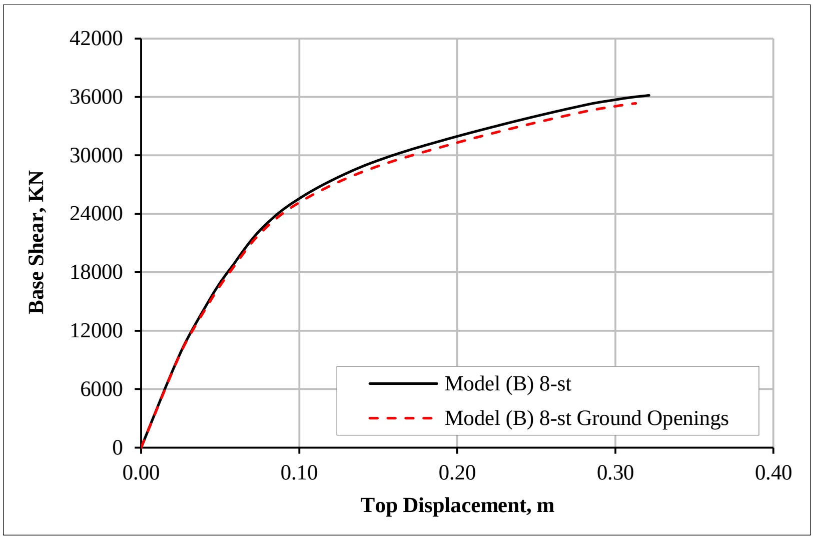

Figure 32. Models Type (B) - 8 Storey

The previous figures present the degradation in base shear related to the same displacement while the opening was conducted on the ground floor. Table 14 presents the calculations of the R-factor by using the acceptance criteria limits for the hinge deformation method.

Table 14. Calculation of R according to Acceptance Criteria Limits for Hinges Deformation (Wall segment)

Model	Time Period	Δu	Δy	μ	Rμ	Vy	Vd	Vu	Rs	R
	(sec)	m	m			kN	kN	kN		
1-A (16-Story)	1.656	0.62	0.28	2.24	2.24	25459.83	11533.00	36713.35	2.21	4.94
5-A (16-Story)	1.665	0.62	0.38	1.65	1.65	29674.03	13509.00	36454.14	2.20	3.62
1-B (8-Story)	0.632	0.24	0.10	2.33	2.03	25957.97	9467.39	33737.89	2.74	5.56
5-B (8-Story)	0.638	0.181	0.104	1.74	1.62	25528.06	11049.00	30428.81	2.31	3.74

Figure 33 presents the relationship between the R-Factor evaluated for the original models and after conducting ground openings with dimensions of 1.8 m in width and 2.75 m in height. Conducting openings on the ground floor had a significant impact on the reduction factor:

- The ground openings have a critical influence on the R-factor.
- In the 16-storey model, the R-factor was reduced by 1.32 as the R-value went from 4.94 to 3.62, while in the 8-storey model, the R-factor was reduced by 1.82 as the R-value decreased from 5.56 to 3.74.

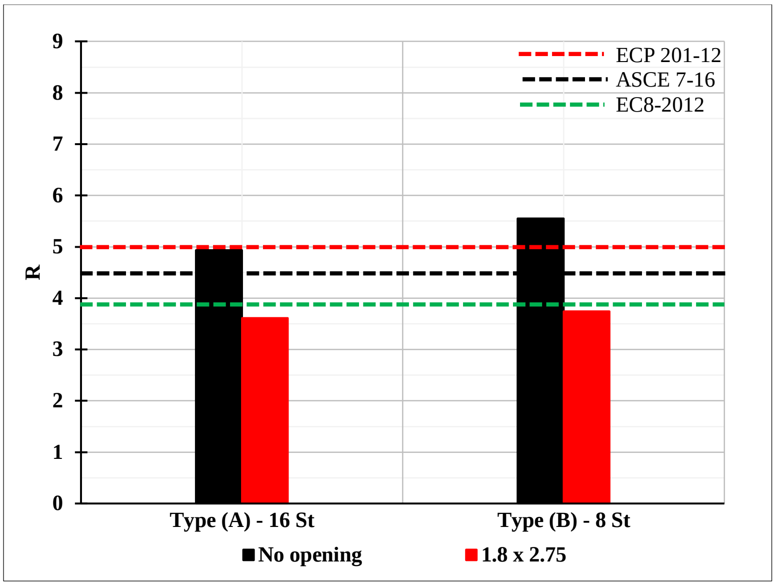

Figure 33. Relation between R and ground opening Dimension in different models

11. Conclusions

A study of the literature was undertaken on some recent research that used finite element simulation and experimental tests to assess the impact of opening on the behaviour of reinforced concrete shear walls. The seismic reactions and stiffness of buildings are impacted by the size of the apertures and their positions in the reinforced shear wall, according to the key findings of this research. Also, multi-story dual-system structures designed according to the Egyptian code of loads, ECP-201 (2012), and checked according to EC8 (2004) [29] were studied. The seismic response modification factor was calculated for shear walls with and without openings. A verified comparison example with eight stories is presented. Then, under Egyptian standards, a numerical study was carried out on four different models of shear wall with and without openings in limited ductility multi-story dual system structures. The following are some of the work's most important outcomes:

- The use of finite element software such as ETABS and SAP2000 to estimate the nonlinear seismic performance of RC concrete structures has been validated by previous numerical studies. Shear and displacement are nearly equivalent in ultimate and yield base shear.
- The findings of three distinct approaches for calculating the seismic response modification factor from the pushover curve have an average difference of less than 10%. Specifically, ASCE41-13 Idealized bilinear curve, Acceptance criterion limit for hinge deformation, Park definition for ultimate and yield steps, and Park definition for ultimate and yield steps.
- The opening area and the response reduction factor have an inverse relationship. The R-factor decreases as the opening area increases. The influence of the opening height on the response reduction factor is larger than the impact of the opening width.
- When the ratio between opening sizes and the area of the shear walls is greater than 20%, the response reduction factor (R) is affected, and the value for the response reduction factor is reduced more than the suggested code.
- The percentage reduction in R-Factor increased as the number of stories increased.
- To enhance the system's performance in the event of an opening. On either side of the opening, half of the reinforcing bars terminating to conduct openings have been inserted, resulting in a 12 percent increase in the response reduction factor.
- Conducting ground-storey openings decreases the response reduction factor by 15% to 30%.
- The given value of R-factor at ECP-201 (2012) equals 5.0 for the limited ductility class of reinforced concrete dual systems from moment resisting frames and shear wall structures with openings, which is an un-conservative value as the accurate value of R-factor is less than the given value.

It’s recommended that the value of R-factor for the limited ductility class of reinforced concrete dual systems from moment resisting frames and shear wall structures in ECP-201 (2012) and EC8 (2004) be changed to the used value in (ASCE7-2016) and (IBC-2018). It may be noted that the American Society of Civil Engineers (ASCE7-2016) and the International Building Code (IBC-2018) specify values for the R-factor of 3.0 for ordinary reinforced concrete moment frames.

12. Declarations

12.1. Author Contributions

Conceptualization, N.E.N., M.N.F., G.H. and A.M.E.; methodology, N.E.N., M.N.F., G.H. and A.M.E.; formal analysis, N.E.N., M.N.F., G.H. and A.M.E.; investigation N.E.N., M.N.F., G.H. and A.M.E.; writing—original draft preparation, N.E.N., M.N.F., G.H. and A.M.E.; writing—review and editing, N.E.N., M.N.F., G.H. and A.M.E. All authors have read and agreed to the published version of the manuscript.

12.2. Data Availability Statement

The data presented in this study are available on request from the corresponding author.

12.3. Funding

The authors received no financial support for the research, authorship, and/or publication of this article.

12.4. Conflicts of Interest

The authors declare no conflict of interest.

13. References

[1] Li, B., Qian, K., & Wu, H. (2016). Flange effects on seismic performance of reinforced concrete squat walls with irregular or regular openings. Engineering Structures, 110, 127–144. doi:10.1016/j.engstruct.2015.11.051.

[2] ECP-201. (2012). Egyptian code for calculating loads and forces in structural work and masonry, Housing and Building National Research Center. Ministry of Housing, Utilities and Urban, Giza, Egypt.

[3] ETABS Computer Software Package (2021). Computer & Structures Inc. Structural Analysis Programs, CSI Inc., California, United States.

[4] SAP2000 (2021). Integrated Software for Structural Analysis and Design, Computers & Structures, Inc., Berkley, United States.

[5] Yasser, I., Saleh, A., Fayed, M., & Naguib, M. (2018). Response modification factor (R) – The Least understandable in Seismic Codes. 15th International Conference on Structural and Geotechnical Engineering (ICSGE15), 10-13 March 2018, Cairo, Egypt. (Advancements in Construction Techniques).

[6] Marsono, A. K., & Hatami, S. (2016). Analysis of reinforced concrete shear walls with single band of octagonal openings. KSCE Journal of Civil Engineering, 20(5), 1887–1894. doi:10.1007/s12205-015-0512-z.

[7] Wallace, J. W., Massone, L. M., Bonelli, P., Dragovich, J., Lagos, R., Lüders, C., & Moehle, J. (2012). Damage and implications for seismic design of RC structural wall buildings. Earthquake Spectra, 28(SUPPL.1), 281–299. doi:10.1193/1.4000047.

[8] Savill, J. S., Wyllie, A. H., Henson, J. E., Walport, M. J., Henson, P. M., & Haslett, C. (1989). Macrophage phagocytosis of aging neutrophils in inflammation. Programmed cell death in the neutrophil leads to its recognition by macrophages. Journal of Clinical Investigation, 83(3), 865–875. doi:10.1172/JCI113970.

[9] Khatami, S. M., Mortezaei, A., & Rui, C. B. (2012). Comparing effects of openings in concrete shear walls under near-fault ground motions. 15th World Conference on Earthquake Engineering (15WCEE), Lisbon, Portugal, 24-28 September 2012, 1, 173-182.

[10] Chowdhury, S., A. Rahman, M., J. Islam, M., & K. Das, A. (2012). Effects of Openings in Shear Wall on Seismic Response of Structures. International Journal of Computer Applications, 59(1), 10–13. doi:10.5120/9511-3901.

[11] Rajesh, M. N., & Prasad, S. K. (2014). Seismic Performance Study on RC Wall Buildings from Pushover Analysis. International Journal of Research in Engineering and Technology, 03(18), 165–171.

[12] Itware, V. A., & Kalwane, U. B. (2015). Effects of openings in shear wall on seismic response of structure. Journal of Engineering Research and Applications, 5(7), 41-45

[13] Sharma, R., & Amin, J. A. (2015). Effects of opening in shear walls of 30- storey building. Journal of Materials and Engineering Structures, 2(1), 44–55.

[14] Gandhi, B. H. (2015). Effect of opening on behaviour of shear wall. International Journal for Technological Research in Engineering, 3(4), 875-878.

[15] Kankuntla, A., Sangave, P., & Chavan, R. (2016). Effects of Openings in Shear Wall. IOSR Journal of Mechanical and Civil Engineering (IOSR-JMCE), 13(1), 1–6.

[16] Jagadale, S. H., & Shelke, N. L. (2016). Analysis of Various Thicknesses of Shear Wall with Opening and without Opening and their Percentage Reinforcement. International Journal of Research in Engineering, Science and Technologies, 2(1), 212-218.

[17] Khatavkar, A. S., Ghadi, A. P., & Barbude, P. A. (2015). Comparitive Study of Response Reduction Factor for Reinforced Concrete and Steel Frame. International Journal of Computer Applications: Special Issue International Conference on Quality Up-gradation in Engineering, Science and Technology (ICQUEST2015), 12-14.

[18] Swetha, K. S., & Akhil, P. A. (2017). Effect of Openings in Shear Wall. International Research Journal of Engineering and Technology, 4(5), 1601-1606.

[19] Hosseini, H. (2017). Numerical Analysis of High Rise Building with Openings on Shear Wall. American Journal of Engineering Research, 2(2), 144–173.

[20] Zhang, Y. (2018). Behavior of reinforced concrete walls with circular openings. PhD Thesis, Department of Civil, Construction, and Environmental Engineering, Iowa State University, Ames, United States.

[21] Yadav, A., Patil, V., & Takkalaki, S. (2019). Analysis of Tall Structures with and without Openings in Shear Walls. International Journal of Innovative Science, Engineering & Technology, 6(5), 36-42.

[22] Alimohammadi, H., Esfahani, M. D., & Yaghin, M. L. (2019). Effects of openings on the seismic behavior and performance level of concrete shear walls. International Journal of Engineering and Applied Sciences, 6(10). doi:10.31873/ijeas.6.10.10.

[23] Ma'moun, K. (2020). Evaluation of response Modification Factor of The Reinforced Concrete Structures with Shear Walls Having Different Sizes of Openings against the Lateral Loading. Master Thesis, Graduate School of Applied Science of Near east University, Nicosia, North Cyprus.

[24] Varma, V. N. K., & Kumar, U. P. (2021). Seismic response on multi-storied building having shear walls with and without openings. Materials Today: Proceedings, 37, 801–805. doi:10.1016/j.matpr.2020.05.827.

[25] Zhang, Y., Yuan, G., Shu, Q., Zhu, M., & Lu, L. (2022). Investigation on seismic behavior of RC shear walls with multiple post-construction openings based on experiment and simulation. Journal of Building Engineering, 46, 103707. doi:10.1016/j.jobe.2021.103707.

[26] Fares, A. M. (2021). The impact of RC shear wall openings at the lateral stiffness of the cantilever shear walls. Research on Engineering Structures and Materials, 7(1), 51–63. doi:10.17515/resm2020.208st0816.

[27] I.S. 1893 (Part 1). (2002). Indian Standard Criteria for Earthquake Resistant Design of Structures Part 1: General Provisions and Buildings (5^{th} Ed.). Bureau of Indian Standards, New Delhi, India. Available online: https://law.resource.org/pub/in/bis/S03/is.1893.1.2002.pdf (accessed on January 2022).

[28] ASCE/SEI7-05. (2005). Supplement to Minimum Design Loads for Buildings and Other Structures, American Society of Civil Engineering, Virginia, United States. doi:10.1061/9780784408094.sup.

[29] BS EN 1998-1. (2005). Eurocode 8: Design of structures for earthquake resistance. General rules, Seismic actions and rules for buildings, London, United Kingdom. doi:10.3403/03244372.

[30] ATC-19. (1995). Structural Response Modification Factors, Applied Technical Council, California Seismic Safety Commission, Redwood City, California, United States.

[31] Borzi, B., & Elnashai, A. S. (2000). Refined force reduction factors for seismic design. Engineering Structures, 22(10), 1244–1260. doi:10.1016/S0141-0296(99)00075-9.

[32] Rahem, A., Djarir, Y., Noureddineb, L., & Tayeb, B. (2021). Effect of Masonry Infill Walls with Openings on Nonlinear Response of Steel Frames. Civil Engineering Journal, 7(2), 278–291. doi:10.28991/cej-2021-03091653

[33] FEMA 273. (1997). NEHRP Guidelines for the seismic Rehabilitation of Buildings. Federal Emergency Management Agency (FEMA), Washington, United States.

[34] FEMA 356. (2000). Prestandard and Commentary for the Seismic Rehabilitation of Buildings. Federal Emergency Management Agency (FEMA), Washington, United States.

[35] FEMA 451. (2006). NEHRP Recommended Provisions for Seismic Regulations for New Buildings and Other Structures and Accompanying Commentary and Maps, Federal Emergency Management Agency (FEMA), Washington, United States.

[36] Park, R. (1989). Evaluation of ductility of structures and structural assemblages from laboratory testing. Bulletin of the New Zealand Society for Earthquake Engineering, 22(3), 155–166. doi:10.5459/bnzsee.22.3.155-166.

[37] Mwafy, A. M., & Elnashai, A. S. (2002). Calibration of force reduction factors of RC buildings. Journal of Earthquake Engineering, 6(2), 239–273. doi:10.1080/13632460209350416.

[38] FEMA 303. (1997). NEHRP Recommended Provisions for Seismic Regulations for New Buildings and Other Structures- Part 2: Commentary. Federal Emergency Management Agency (FEMA), Washington, United States.

[39] Newmark, N. M., & Hall, W. J. (1982). Earthquake spectra and design. Engineering monographs on earthquake criteria, Structural design, and strong motion records (1^{st} Ed.). Earthquake Engineering Research Institute, Oakland, United States.

[40] ASCE 41-13. (2014). Seismic Evaluation and Retrofit of Existing Buildings. American Society of Civil Engineers, Reston, United States. doi:10.1061/9780784412855.

[41] IBC2018. (2018). International building Code 2018. International Code Council, Washington, United States.

[42] ASCE/SEI 7-16 (2017). Minimum Design Loads for Buildings and Other Structures. American Society of Civil Engineers, Reston, United States. doi:10.1061/9780784414248.

[43] Vojdan, B. M., & Aghayari, R. (2017). Investigating the seismic behavior of RC shear walls with openings strengthened with FRP sheets using different schemes. Scientia Iranica, 24(4), 1855–1865. doi:10.24200/sci.2017.4276.

[44] Miao, Z. W., Lu, X. Z., Jiang, J. J., & Ye, L. P. (2006). Nonlinear FE Model for RC Shear Walls Based on Multi-Layer Shell Element and Micro-Plane Constitutive Model. Computational Methods in Engineering & Science, 204–204. doi:10.1007/978-3-540-48260-4_50.

[45] ATC-40. (1996). Seismic evaluation and retrofit of concrete buildings. Applied technology Council, California Seismic Safety Commission, Redwood city, United States.

[46] ASCE (2017b). Seismic Evaluation and Retrofit of Existing Buildings. Seismic Evaluation and Retrofit of Existing Buildings. American Society of Civil Engineers, Reston, Virginia.

[47] ACI 318-02/318R-02. (2002). Building code requirements for structural concrete: (ACI 318-02) and commentary (ACI 318R-02). American Concrete Institute, Farmington Hills, United States.